

AD-A083 992

MASSACHUSETTS INST OF TECH LEXINGTON LINCOLN LAB
PIN DIODE WEIGHT CIRCUITS. (U)

DEC 79 B M POTTS

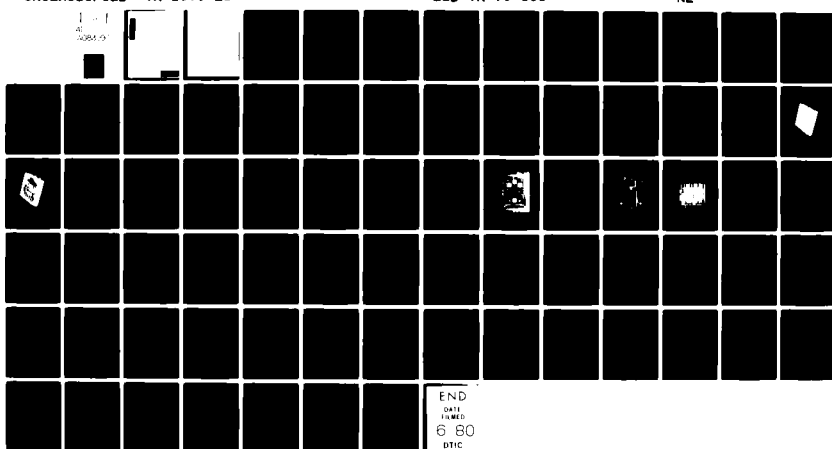
UNCLASSIFIED TN-1979-26

F/6 9/5

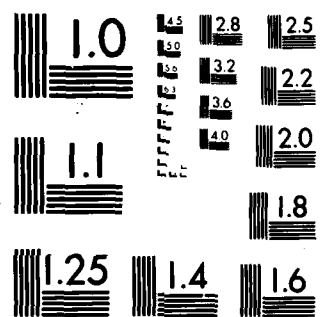
F19628-80-C-0002

NL

ESD-TR-79-306



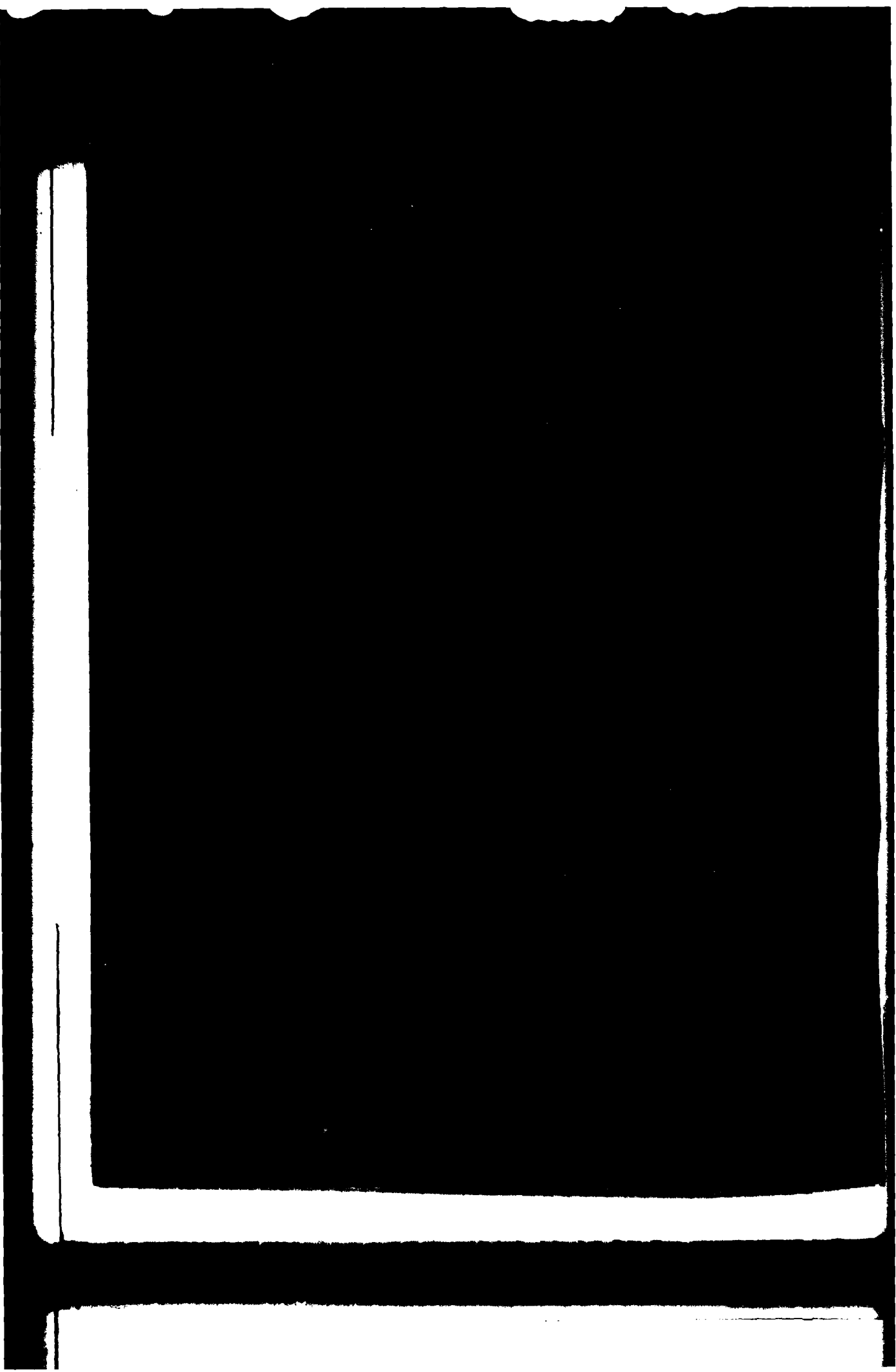
END
DATE
FILED
6 80
DTIC



MICROCOPY RESOLUTION TEST CHART
NATIONAL BUREAU OF STANDARDS-1963-A

ADA 083992

5 5 105



**MASSACHUSETTS INSTITUTE OF TECHNOLOGY
LINCOLN LABORATORY**

PIN DIODE WEIGHT CIRCUITS

B. M. POTTS
Group 61

TECHNICAL NOTE 1979-26

28 DECEMBER 1979

Approved for public release; distribution unlimited.

LEXINGTON

MASSACHUSETTS

ABSTRACT

This report is one of a number of technical notes describing various aspects of the design, fabrication, and performance of a demonstration analog feedback processor. In this report we examine the PIN diode weight circuits which are used in the adaptive processor to control the attenuation and phase of the eight signal channels which make up the processor. The weighting circuits are required to have well-matched transfer functions which track closely from channel to channel so as not to degrade the processor cancellation. To achieve the necessary tracking performance, two different weight circuit designs were investigated. The tracking performance of the first set was found to be limited by the direct feed-through of input signals to the output of the weight circuit as a result of the limited dynamic range of the weight circuit attenuator. To overcome this limitation, a second set of weight circuits having significantly improved tracking characteristics was fabricated using an improved attenuator circuit design.

Information relevant to the design, fabrication and testing of each weight circuit is presented along with measured data to demonstrate its performance. Techniques used in characterizing the frequency tracking performance of multiple weight circuits are discussed and measurement data is presented to illustrate the relative tracking performance of the weight circuits.

Accession for NTIS Gen. I	<input checked="" type="checkbox"/>
DOC TAB	<input type="checkbox"/>
Unannounced	<input type="checkbox"/>
Justification	<input type="checkbox"/>
By _____	
Distribution	
Availability Code	
Dist.	Available or special

CONTENTS

Abstract	iii
Illustrations	vi
Tables	viii
I. INTRODUCTION	1
II. DESIGN REQUIREMENTS	4
III. DESIGN APPROACH	8
IV. WEIGHT CIRCUIT DESCRIPTIONS	13
4.1 Narrowband Weight Circuits	13
4.2 Broadband Weight Circuits	20
V. SINGLE WEIGHT PERFORMANCE	31
5.1 Narrowband Weight Circuits	31
5.2 Broadband Weight Circuits	37
VI. WEIGHT TRACKING PERFORMANCE	43
6.1 Measurement Techniques	43
6.2 Measurement Results	51
VII. SUMMARY OF RESULTS	63
Acknowledgments	65
References	66

ILLUSTRATIONS

1.	Simplified Block Diagram of an 8-Channel Analog Feedback Adaptive Processor	2
2.	Parametric Representation of the Tracking Error σ^2 vs Amplitude and Phase Mismatch, $20 \log_{10}(1+\sigma_a)$ and σ_ϕ , Respectively (after Mayhan [9])	7
3.	Weight Circuit using Fixed Phase Shifters, Four Attenuators and One Four-Way Combiner	9
4.	Weight Circuit using Fixed Phase Shifters, Two Attenuators, Two Biphase Modulators and One Two-Way Combiner	10
5.	Attenuator/Modulator Circuit used in the Narrowband PIN Diode Weight Circuit	14
6.	Narrowband PIN Diode Weight Circuit with Top Cover Removed to Illustrate the RF Circuit	18
7.	Narrowband PIN Diode Weight Circuit with Bottom Cover Removed to Illustrate the Driver Circuit	19
8.	Broadband Attenuator/Modulator Circuit Consisting of a Double Pi Attenuator and a Double Balanced Mixer Operated as a Biphase Modulator	21
9.	Variable Resistance Pi Attenuator Circuit	22
10.	Schematic Diagram of the Double Pi Attenuator Circuit used in the Broadband PIN Diode Weight Circuit	25
11.	Broadband RF Weight Module	27
12.	Front Side View of Broadband PIN Diode Weight Circuit Showing RF Weight Module and Two-Way Divider	29
13.	Rear Side View of Broadband Pin Diode Weight Module Showing Driver Circuit	30
14.	Attenuation and Phase Response of the "I" Channel of Weight #2 vs Control Voltage, V_I , at 125 MHz	32

ILLUSTRATIONS (Cont'd)

15. Intermodulation Measurements for Narrowband Weight Circuit	34
16. Weight Attenuation vs Frequency Obtained by Adjusting Weight for Maximum Attenuation and Sweeping Frequency.	36
17. Attenuation, Return Loss and Phase Shift as a Function of Control Voltage at 121.4 MHz for a Double Pi Attenuator Circuit	38
18. Attenuation vs Frequency for Double Pi Attenuator for Variable Control Voltages	40
19. Intermodulation Performance vs Attenuation for Double Pi Attenuator	41
20. Intermodulation vs Attenuation for Broadband Weight Circuit	42
21. Automated Test Set-Up for Characterizing Weight Tracking Performance	44
22. Measurements Conducted on a Single Narrowband Weight Circuit Illustrating Weight Attenuation vs Number of Iterations for Selected Values of μ and ϵ	52
23. Comparison of Measured Tracking Data for Narrowband Weights Showing Null Depth vs Frequency for 1, 2 and 4 Weights	54
24. Comparison of Measured Tracking Data for Broadband Weights Showing Null Depth vs Frequency for 1, 2 and 4 Weights	56
25. Cancellation Performance Obtained from 40 Random Selections of the Beam Steering Vector and Reference Channel	58
26. Eigenvalues vs Bandwidth for the Eight Broadband Weight Circuits, Measured using a Fixed Control Voltage $V_I=0$, $V_Q=1$ Volt	60
27. Comparison of the Eigenvalue Ratio, s_2/s_1 , for the Narrowband and Broadband Weights vs Bandwidth	61

TABLES

1. Weight Circuit Design Requirements/Goals	5
2. Series and Shunt Resistance Values for a Pi-Attenuator Circuit vs Attenuation	23
3. Comparison of Cancellation over 10 MHz Bandwidth as a Function of the Number of Weights	57
4. Comparison of PIN Diode Weight Circuit Performance over 10 MHz IF Bandwidth Centered at 121.4 MHz	64

I. INTRODUCTION

In this technical note we examine two types of PIN diode weight circuits which are capable of producing controlled attenuation and phase shift (continuous from 0° to 360°). Both circuits were designed for used in the analog feedback adaptive processor* shown in block diagram form in Fig. 1. The processor consists of eight "identical" signal paths or channels with each channel containing a separate RF front-end section, an RF to IF converter, amplifier and filter chain, and a weight circuit. The weight circuits, which are implemented at IF (~ 121 MHz), provide the capability of changing the amplitude and/or phase of the signal in each channel using control voltages generated in the Correlation and Weight Control Unit (A7). After weighting, the various signal channels are combined in an 8-way combiner to form the processor output signal.

The adaptive processor in Fig. 1 uses a variation of the least mean square (LMS) algorithm discussed by Gabriel^[1] for controlling the weight circuits. This modification allows for the incorporation of "beam steering" signals into the feedback loops for controlling the transfer function of the processor in the absence of any interference signals. For our application the processor is used to control an antenna radiation pattern so that the beam steering signals, in this case, determine the quiescent or unadapted radiation pattern of the antenna.

Since the LMS algorithm is a power minimization algorithm, the weight circuits are adjusted to minimize the output power, with signals being distinguished on the basis of their relative power level. When the input signal levels are less than the loop threshold, the weight settings, and hence the processor input/output transfer function, are determined by the "beam steering" signals. This is the normal situation when only user signals are present at the inputs to the processor. However, as the input signal level to the processor increases such as, for example, when a large interference source is present, the feedback loops sense the increase in output power level and respond by generating the appropriate weight control voltages to minimize the output signal level.

* A third set of weight circuits utilizing transconductance multipliers were also tested with the adaptive processor, and are discussed separately in Ref. [7].

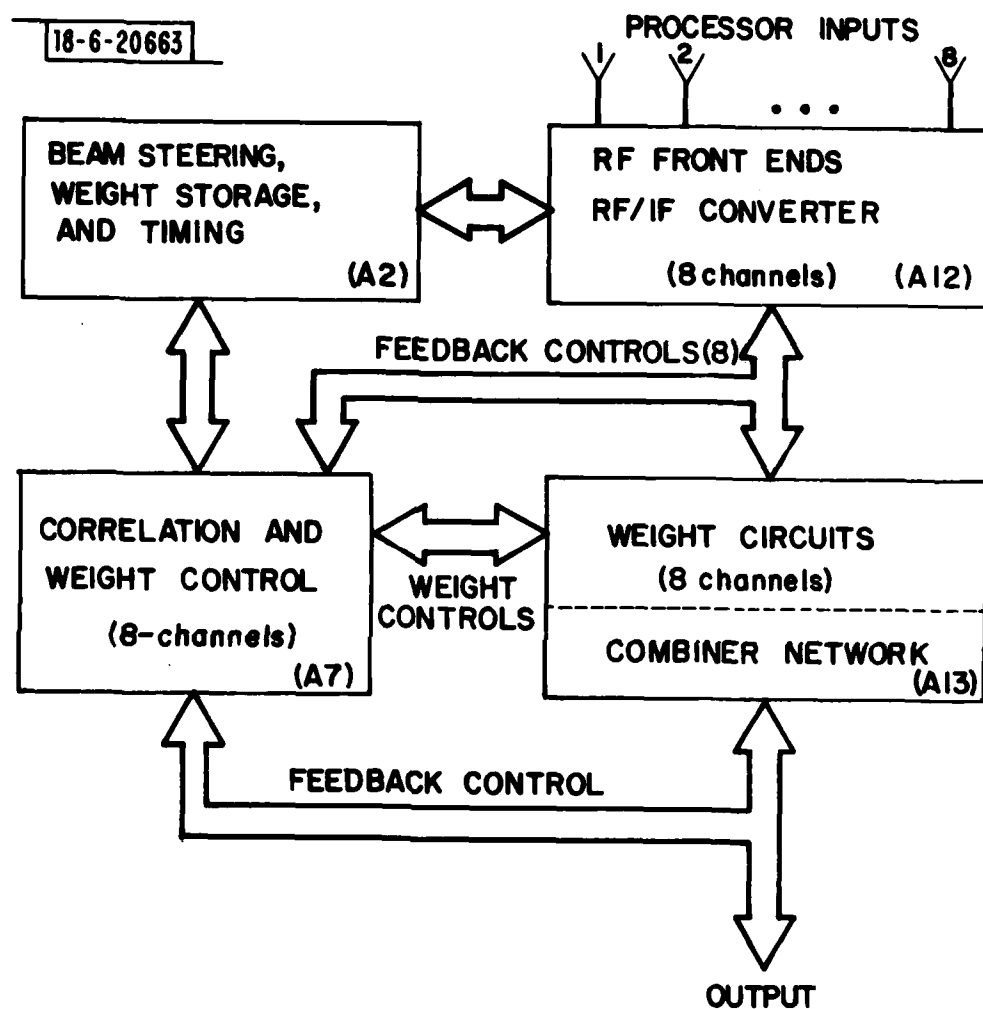


Fig. 1. Simplified block diagram of an 8-channel analog feedback adaptive processor.

In this fashion, by distinguishing signals on the basis of their power level, the processor is able to adaptively control its transfer function so that signals above the loop threshold level (i.e., interference signals) are attenuated, and the output power is minimized while signals below the loop threshold (i.e., user signals) are unattenuated.

A detailed description of the processor, its performance and its various subsystems are discussed in other technical notes^[2-8]. In this technical note we discuss only the PIN diode weight circuits. Section II describes the weight circuit design requirements which is followed, in Section III, with a general discussion of several candidate weight circuit configurations. Details relating to the weight circuit fabrication, testing and performance are presented in the remaining sections.

II. DESIGN REQUIREMENTS

The weighting circuits are designed to operate over a minimum bandwidth of 10 MHz centered at an IF frequency of approximately 121.4 MHz. The eight weighting circuits (one for each channel of the processor) are designed to adjust the amplitude and/or phase of the signal in each channel in accordance with a pair of control voltages, denoted by V_I and V_Q , which control the real and imaginary components of the weight, respectively. In Table 1 are summarized the principal design requirements of the weighting circuits. It should be noted that the transfer function of each weight circuit must be matched and made to track from unit to unit over the IF bandwidth. For an ideal processor, the frequency transfer characteristics of all channels would be identical, resulting in a cancellation which is independent of frequency. In practice, however, the signal channels cannot be made exactly the same due to inherent mismatches in the components which make up the channels. As a result, the cancellation bandwidth over which the adaptive processor is able to achieve a specified interference cancellation depends upon how closely the frequency characteristic of the channels can be made the same. For the weight circuits, perfect tracking of the transfer functions implies that the transfer function of each weight circuit must be either invariant with frequency or track exactly from unit to unit, independent of the weight setting and input power level. Although neither of these conditions can be satisfied exactly and therefore perfect cancellation can never be achieved over a finite bandwidth, one can, however, specify how well the channels must be matched in amplitude and phase to achieve a given level of cancellation. One method of doing this is the technique described by Mayhan^[9] and Hodson^[10] in which the processor performance (i.e., its cancellation level) is expressed in terms of the rms channel mismatch errors. For the case in which the channel tracking errors are uncorrelated and approximately the same from channel to channel, the cancellation level can be expressed as

$$C \approx \sigma^2 = \sigma_A^2 + \sigma_\phi^2 \quad (2.1)$$

TABLE 1
WEIGHT CIRCUIT DESIGN REQUIREMENTS/GOALS

Center Frequency	121.4 MHz
Bandwidth	10 MHz
Input/Output VSWR	< 1.22 (return loss >20 dB)
Max Input Power Level	0 dBm
Dynamic Range	> 40 dB
Phase	Continuous from 0° to 360°
Weight Tracking Performance	Sufficient to produce greater than -40 dB cancellation over the bandwidth when two or more weights are adjusted to cancel at 121.4 MHz
Weight Control Signals	Controllable from two analog voltages, each operating over -1 to +1 volts for the control of the real and imaginary components, respectively
Weight Response	Weight attenuation should be linear with control voltage such that weight magnitude, $W \sim [V_I^2 + V_Q^2]^{1/2}$
Control Signal Bandwidth	< 100 KHz
Third Order, Two-Tone Intermodulation Intercept	+15 dBm, min. at output ($W = 1$)

where σ_A and σ_ϕ represent the standard deviations of the amplitude and phase, respectively, of the channel tracking errors. In the context used here, cancellation is defined as the ratio of the interference to thermal noise ratio at the output before and after adaption, that is,

$$C \equiv \frac{(I/N)_a}{(I/N)_b} \quad (2.2)$$

where the subscript "a" denotes "after" adaption and "b" denotes "before" adaption. Shown in Fig. 2 is a parametric representation of cancellation (assuming $C = \sigma^2$) vs $20 \log(1 + \sigma_A^2)$ and σ_ϕ to illustrate the tight tolerances required to achieve high values of cancellation. Thus to achieve -40 dB of cancellation, as an example, requires that the rms amplitude and phase variations between channels be no more than 0.09 dB and 0.57 degree, respectively. Fig. 2 clearly points out the necessity of matching the N signal flow paths of the processor very closely if large values of cancellation are required.

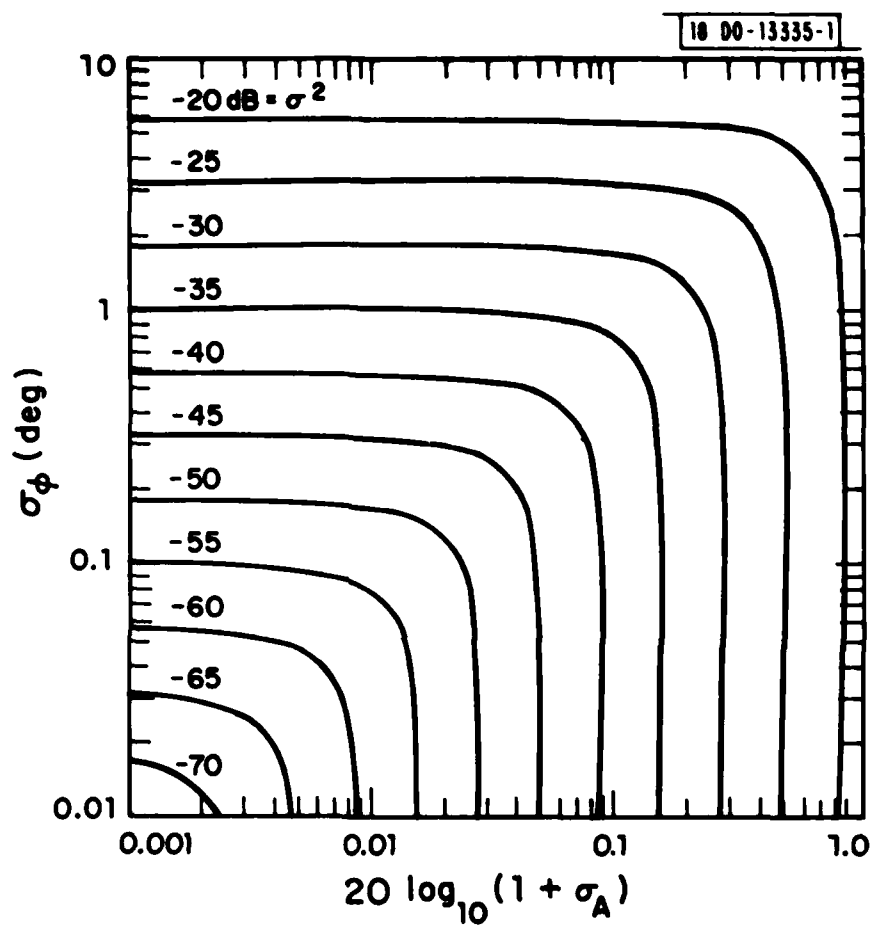


Fig. 2. Parametric representation of the tracking error σ^2 vs amplitude and phase mismatched, $20 \log_{10}(1 + \sigma_A)$ and σ_ϕ , respectively (after Mayhan [9]).

III. DESIGN APPROACH

In order to realize weighting circuits with low levels of mismatch errors, one must carefully consider both the circuit topology and the components used in fabricating the weight circuits. In some applications the weighting function can be accomplished simply by using an attenuator and phase shifter in series. One limitation of this circuit is the inability of the attenuator to turn off completely due to the limited dynamic range of real attenuators. Also, and perhaps more importantly, it is difficult to control this type of weight circuit using control voltages specified as "inphase", V_I , and "quadrature phase", V_Q , rather than in terms of "amplitude" and "phase". It is also very difficult to devise a phase shift circuit which can achieve full phase control (0° to 360°) at these low frequencies with low dispersion. Circuits which produce phase shift directly as a result of changes in time delay (such as in switched delay line phase shifters) generate relatively large time delay mismatches, and consequently are highly dispersive. Other types of phase shift circuits in which phase shifts are produced by reactive loading of transmission lines are also not suited for our application because of their limited phase shift per section, and relatively small bandwidth.

There are other network topologies, however, in which weighting can be achieved without the necessity of producing phase shift directly. For example, complex weighting can be accomplished using fixed power division and fixed phase shifts and only one variable component, an attenuator. Two such circuits for accomplishing this are illustrated in Fig. 3 and Fig. 4. In both of these circuits, complex weighting is accomplished by separating the input signal into a number of nearly equal amplitude, orthogonal phase components. Each component is then attenuated and summed to produce an output signal whose amplitude and phase can be controlled by changing the relative attenuation of each component. The circuit in Fig. 3 does this by generating four components (with relative phases of 0° , -90° , -180° and -270°) which are each separately attenuated and summed to produce, in principle, any desired attenuation or phase shift. However, as a practical matter, the dynamic range of the attenuators and the degree to

18-6-20664

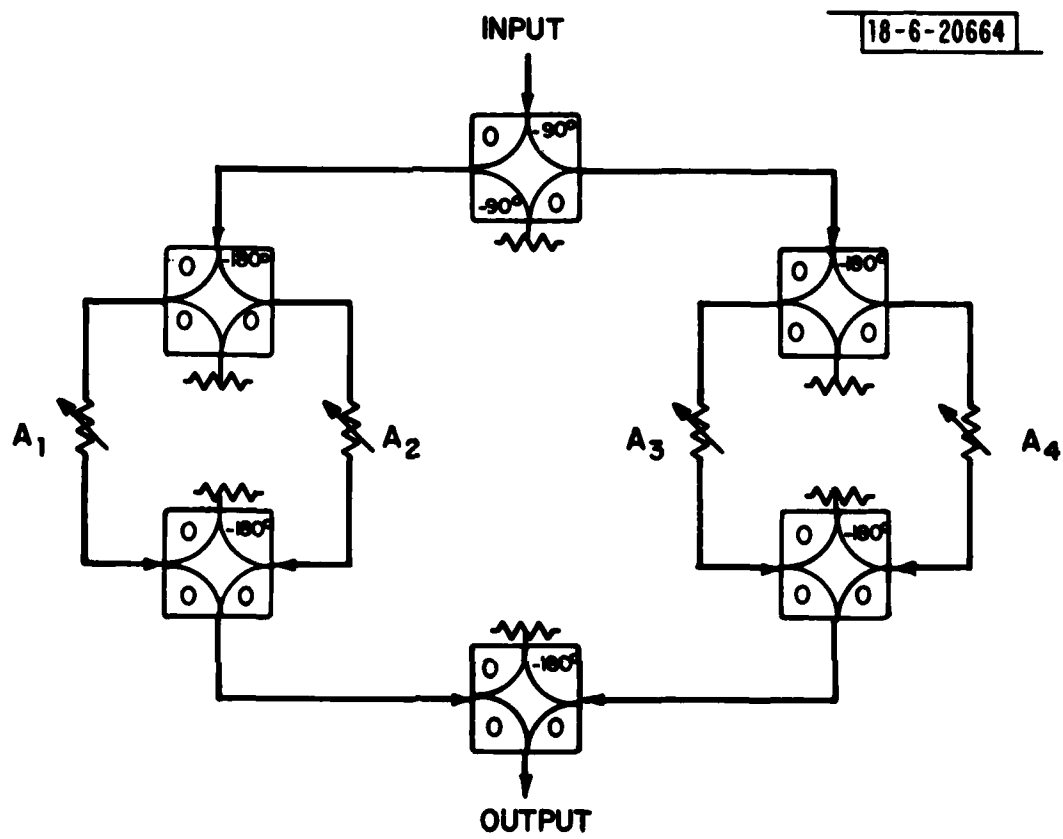


Fig. 3. Weight circuit using fixed phase shifters, four attenuators and one four-way combiner.

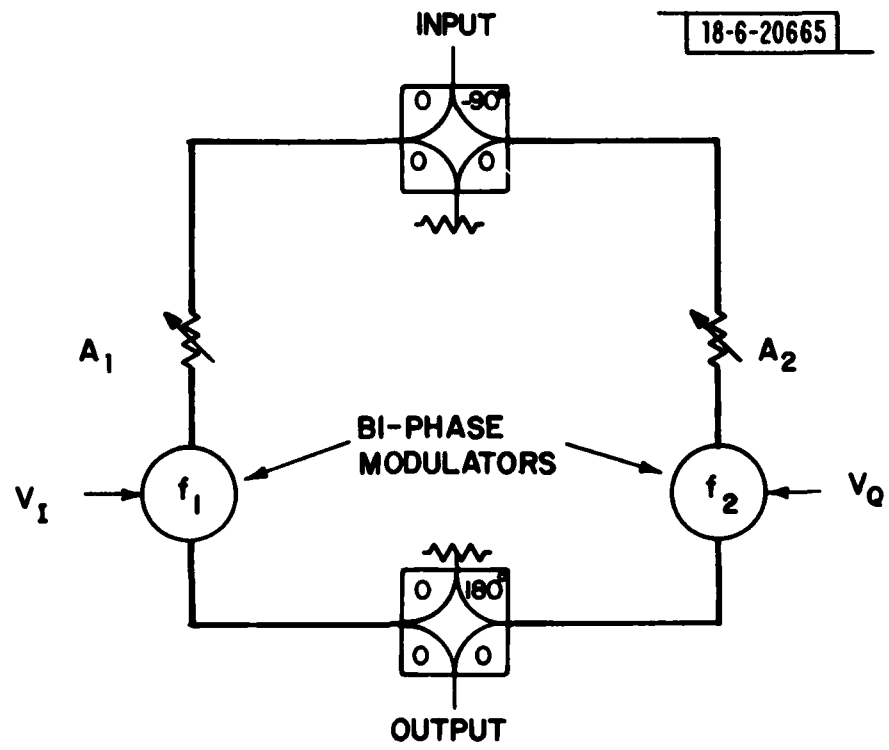


Fig. 4. Weight circuit using fixed phase shifters, two attenuators, two biphasic modulators and one two-way combiner.

to which the frequency response of the attenuators can be matched as a function of frequency will determine the ultimate performance of this circuit. Letting A_1 , A_2 , A_3 , and A_4 , represent the attenuator settings associated with the 0° , -180° , -90° and -270° signal paths, respectively, the magnitude and phase at the output can be written as

$$|W| = \frac{1}{4} [(A_1 - A_2)^2 + (A_3 - A_4)^2)]^{1/2} \quad (3.1)$$

$$\phi = -\tan^{-1} \left[\frac{A_3 - A_4}{A_1 - A_2} \right] \quad (3.2)$$

By choosing

$$A_1 = 1 - |v_I|$$

$$A_2 = |v_I|$$

$$A_3 = 1 - |v_Q|$$

$$A_4 = |v_Q|$$

where $-1 \leq v_I \leq +1$, $-1 \leq v_Q \leq +1$ are the weight control voltages, Eqns. (3.1) and (3.2) reduce to

$$|W| = \frac{1}{4} [(1 - 2|v_I|)^2 + (1 - 2|v_Q|)^2]^{1/2} \quad (3.3)$$

$$\phi = -\tan^{-1} \left[\frac{1 - 2|v_Q|}{1 - 2|v_I|} \right] \quad (3.4)$$

It can be noted from Eqs. (3.3) and (3.4) that although any amplitude or phase shift can be obtained by varying only attenuation, the cost of achieving this flexibility comes about in terms of an increase in circuit loss compared to a direct phase shifter-attenuator weight circuit. Assuming that the magnitude of the weight is always less than unity (i.e., v_I and v_Q cannot both simultaneously have magnitude of one), the minimum insertion loss which will permit any value of phase shift is 12 dB.

A reduction of 6 dB in insertion loss can be obtained, compared to that of Fig. 3, by using an alternate weight circuit design shown in Fig. 4. In this circuit the input signal is divided into two phase quadrature components (with relative phase of 0° and -90°). Each component is attenuated, passed through a biphase modulator (producing a relative phase shift of 0° or 180°) and then summed to produce the output signal whose magnitude and phase are given by

$$|w| = \frac{1}{2} \left[v_I^2 + v_Q^2 \right]^{1/2} \quad (3.5)$$

$$\phi = -\tan^{-1} \left[\frac{f_2 v_Q}{f_1 v_I} \right] \quad (3.6)$$

where we have assumed $A_1 = |v_I|$, $A_2 = |v_Q|$ and

$$f_1 = \begin{cases} +1 & v_I \geq 0 \\ -1 & v_I < 0 \end{cases} \quad (3.7)$$

$$f_2 = \begin{cases} +1 & v_Q \geq 0 \\ -1 & v_Q < 0 \end{cases} \quad (3.8)$$

This circuit is similar to that in Fig. 3 in that it produces four quadrature signals; however, unlike the previous circuit in which all four components are generated simultaneously, only two of the four quadrature components are present in the circuit of Fig. 4 at any one time. The net effect of this is that a single two-way combiner can be used in Fig. 4 as contrasted to the four way combiner in Fig. 3; this results in less combiner loss and a 6 dB reduction in the circuit insertion loss. Consequently, because of its lower loss and use of fewer components, the weight circuit configuration in Fig. 4 was selected for use in the adaptive processor.

IV. WEIGHT CIRCUIT DESCRIPTIONS

The two sets of PIN diode weight circuits which were built and tested in the adaptive processor differ fundamentally in how the attenuator and biphase modulator circuits in Fig. 4 are realized. For discussion purposes we refer to the first set of circuits as narrowband weights in contrast to the second set which were found to have better performance over a much wider bandwidth and are referred to as broadband weights.

4.1 Narrowband Weight Circuits

Fig. 5 illustrates the circuit design for the narrowband weight which combines the functions of the attenuator and biphase modulator. With this circuit attenuation and biphase modulation can both be achieved by controlling a pair of PIN diodes which are connected to the 0° and -90° ports of a quadrature hybrid power divider. With an input signal applied to port A of the hybrid, the output signal at port D is proportional to the magnitude and phase of the reflection coefficients produced by the PIN diodes at ports B and C, i.e.,

$$E_0 \sim -j(\rho_1 + \rho_2) E_{in} \quad (4.1)$$

where E_0 is the output signal, E_{in} the input signal and ρ_1 and ρ_2 the PIN diode reflection coefficients which can be expressed as

$$\rho_{1,2}(I) = \frac{z_{1,2}(I) - z_0}{z_{1,2}(I) + z_0} \quad (4.2)$$

$z_{1,2}(I)$ = PIN diode impedance (function of I)

z_0 = transmission line characteristic impedance

I = diode bias current

Thus by adjusting the diode bias currents, the reflection coefficients can be made to vary from approximately +1 to -1, which corresponds to changing the

18-6-20666

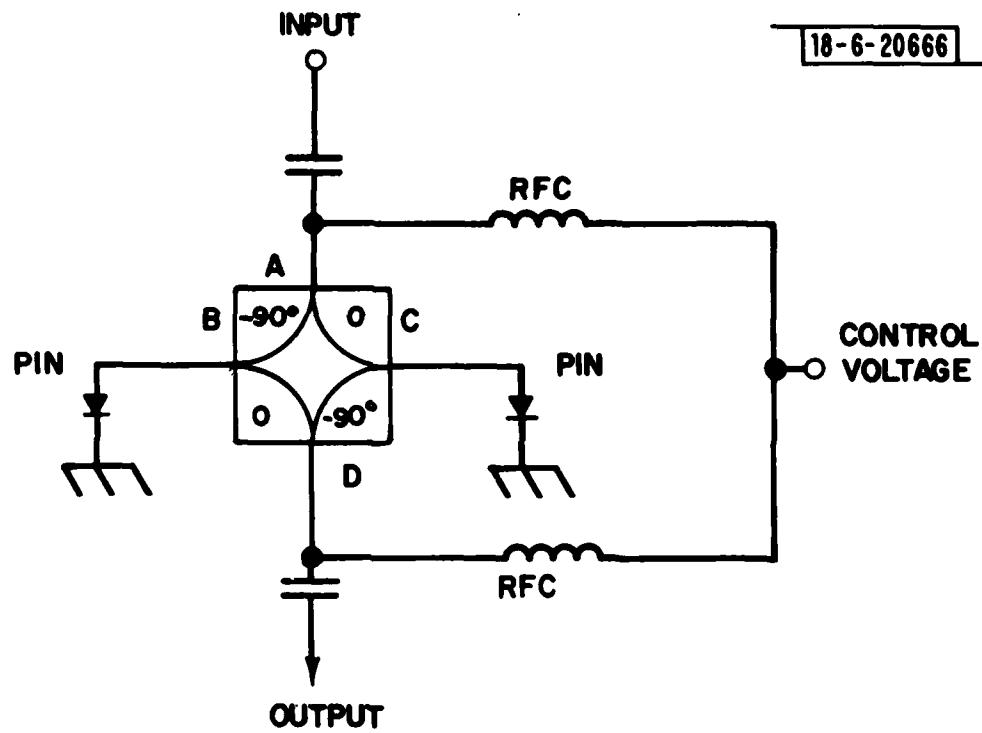


Fig. 5. Attenuator/modulator circuit used in the narrowband PIN diode weight circuit.

diode impedance from a very large value (\sim open circuit) to a small value (\sim short circuit), respectively. Furthermore, reflections from the diodes which propagate toward the input port add out of phase (i.e., $\rho_1 - \rho_2$) resulting in a good impedance match (to the extent that ρ_1 and ρ_2 can be made the same) over the full attenuation range.

The two principal limitations of this particular circuit are its limited dynamic range and narrow bandwidth. To produce a large attenuation requires that the reflection coefficient of both diodes be made small, which in turn requires that the diode impedances be controlled very closely and matched to the characteristic impedance of the transmission line (in this case 50 ohms). Attenuation levels in excess of 40 dB correspond to reflection coefficients less than 0.01, which are difficult to achieve in practice and require that the diode impedance deviate less than ± 0.5 ohm from 50 ohms over the IF bandwidth. A second problem has to do with the fact that the PIN diode, which can be modeled as a variable resistance in parallel with a capacitance, has an effective reactance which changes with attenuation thereby producing an attenuation and frequency dependent phase shift, and degraded tracking performance.

Eq. (4.1) expresses the output of the narrowband attenuator/modulator circuit in terms of the signals reflected by the PIN diodes. These signals are normally referred to as weighted output signals to distinguish them from other spurious, non-weighted signals which also occur at the output due to imperfections in the circuit. We have found that a good model for the narrowband weight circuit is an ideal, frequency independent weight shunted by a non-weighted feed-through path. The amount of feed-through can be characterized by an isolation parameter, $|\gamma|^2$, and a time delay, τ' . In the circuit of Fig. 5, the input-to-output isolation of the hybrid power divider is generally limited to values of 30 to 40 dB and consequently is a primary source of weight feed-through. As a result, there exist signals at the output which "leak" through the hybrid power divider (i.e., the non-weighted signal) and combine with the PIN diode reflected signals (the weighted signals) to produce an output signal given by

$$E_0 = (\rho e^{j\omega\tau} + |\gamma|^2 e^{j\omega\tau'}) E_{in} \quad (4.3)$$

where

ρ = PIN diode reflection coefficients (assumed to be equal)

$|\gamma|^2$ = non-weighted feed-through level (i.e., the hybrid isolation)

τ = time delay of the weighted signal path

τ' = time delay of the non-weighted signal path

The implications of Eq. (4.3) on the weight tracking performance are quite serious unless the non-weighted feed-through signals can be maintained at sufficiently low levels, and the time delay difference, $\Delta\tau = \tau - \tau'$, minimized. Analysis has shown [4] that the frequency variations of the feed-through signals over the nulling bandwidth cannot, in general, be compensated for by the weight control circuitry, and hence the feed-through signals degrade the cancellation level. The amount by which the cancellation level is degraded depends upon the extent to which the feed-through signals are correlated from one weight circuit to another, and for the two cases in which the signals are uncorrelated and correlated the following bounds on the cancellation level are obtained,

$$C = N|\gamma|^2 \delta^2 \quad (\text{uncorrelated})$$

$$C = N^2 |\gamma|^2 \frac{(\pi BW \Delta\tau)^2}{3} \quad (\text{correlated}) \quad (4.4)$$

where

N = number of weight circuits

δ^2 = rms channel tracking error

BW = nulling bandwidth

$\Delta\tau = \tau - \tau'$, time delay between the weighted path and feed-through path

Eq. (4.4) clearly points out the necessity of minimizing weight feed-through, particularly feed-through signals which are correlated from weight to weight such as those arising, for example, from the finite isolation of the hybrid power dividers.

In order to minimize the weight feed-through signals, each narrowband weighting circuit was fabricated using special high-performance lumped element hybrid power dividers selected to have a minimum input-output isolation of 35 dB over the 10 MHz IF bandwidth. Measurements were made by testing various hybrids with selected PIN diodes, and choosing the best combination of diodes and hybrids to maximize the isolation level. With this procedure, isolation levels of 35 to 40 dB were achieved over a 10 MHz bandwidth centered at the IF frequency of 121.4 MHz. Unfortunately, as will be shown later, even these low isolation levels are too large to achieve cancellation levels of 40 dB over bandwidths larger than about five percent.

The eight narrowband weight circuits were assembled in separate modules measuring 5.50 x 5.50 x 1.625 inches. Fig. 6 illustrates the physical layout of a complete weight circuit, with the top cover removed to expose the RF circuit. Located at the input of the RF circuit is a two-way power divider which is used to separate the channel signal into two parts, with one signal being applied to the weight circuit and the other to the analog feedback circuit for control of the weight (see Fig. 1). The components used in fabricating the weight circuits are, for the most part, standard catalog items. The single exception is the quadrature hybrid power dividers which are used in the attenuator circuit; these hybrids were procured separately to meet the special isolation requirements.

The biasing signals for controlling the PIN diodes are supplied by the driver circuit, located on a separate printed circuit card mounted below the RF circuit (see Fig. 7). Included on this card are the linearizer and drive circuits for controlling the "I" and "Q" attenuator/modulation circuits. A three segment diode-resistance shaping network is used as the linearizer

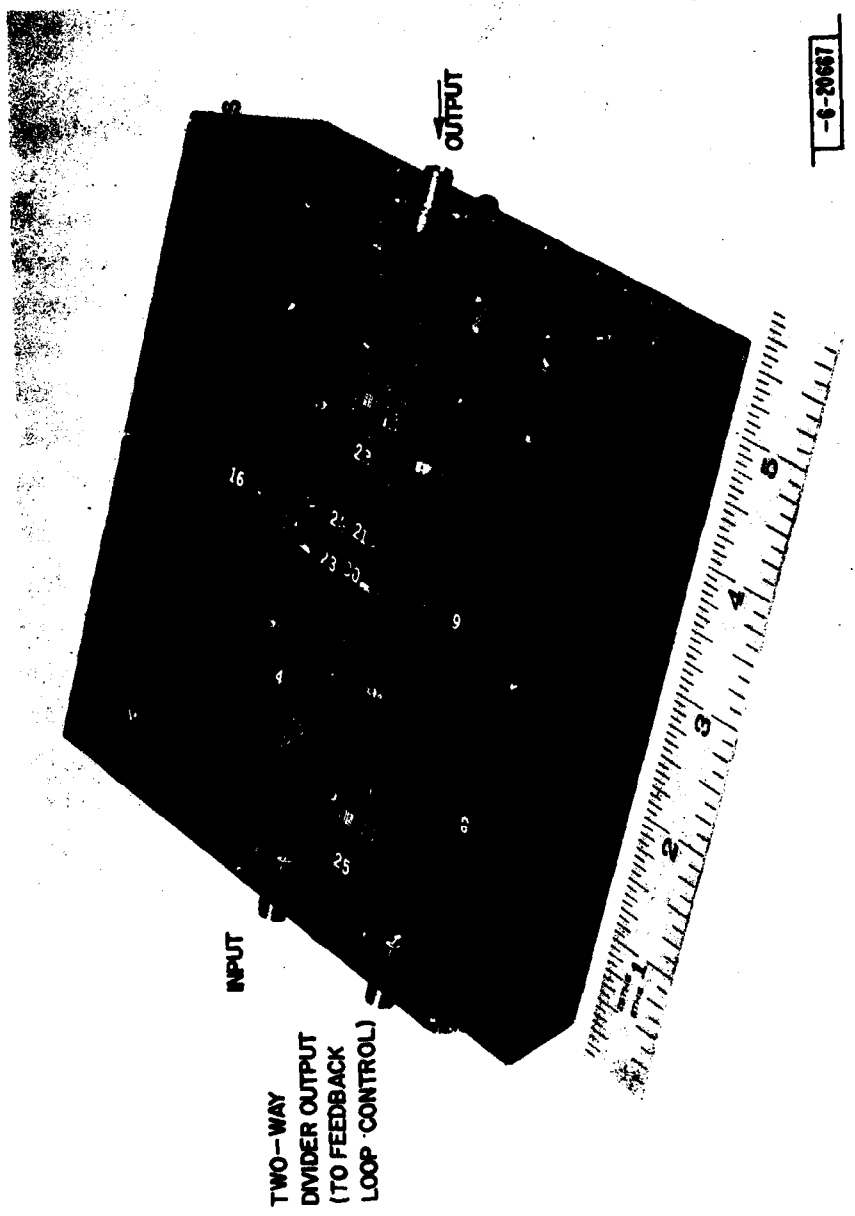


Fig. 6. Narrowband PIN diode weight circuit with top cover removed to illustrate the RF circuit.

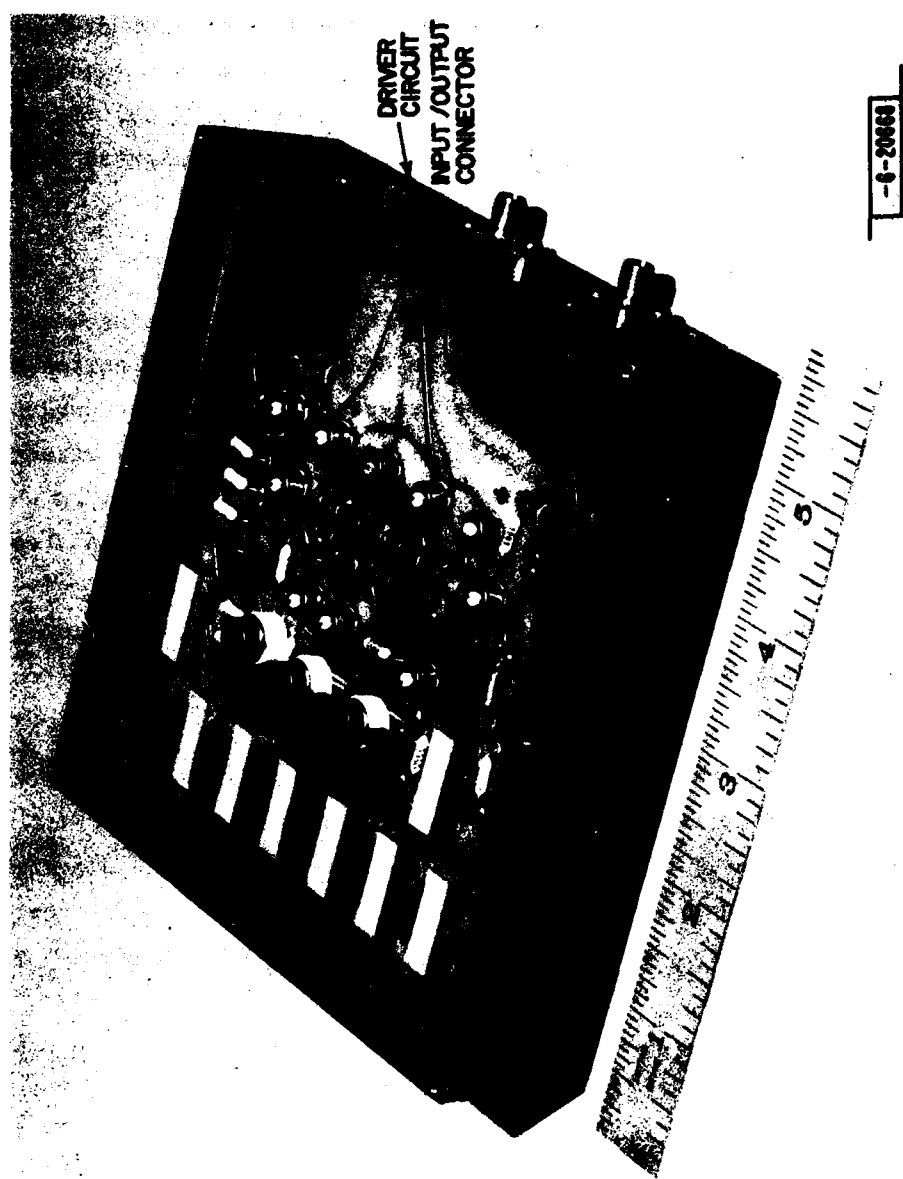


Fig. 7. Narrowband PIN diode weight circuit with bottom cover removed to illustrate the driver circuit.

circuit to partly compensate for the non-linear response of the PIN diodes. With this circuit it is possible to produce attenuation which is a linear function of the control voltage over a range of approximately 30 dB. Beyond 30 dB, the attenuator linearity gradually deteriorates as the weighted signal level approaches the level of the feed-through signals.

4.2 Broadband Weight Circuits

The broadband PIN diode weight circuits are capable of operating over wider bandwidths with improved tracking performance in comparison to the narrowband weight circuits. To obtain this improved performance, the attenuator/modulator circuit was designed as shown in Fig. 8, using a broadband PIN diode attenuator for amplitude control, and a double balanced mixer (operating as a biphase modulator) for 0 or 180° phase control. The attenuator circuit was constructed by cascading two pi attenuators so that each attenuator operates over only one-half of the total dynamic range. Operating the attenuators in this manner reduces the range of impedances over which the PIN diodes operate which tends to minimize phase changes introduced by the varying reactance of the PIN diodes.

Before discussing the PIN diode attenuator circuit let us first describe the operation of the simple resistive pi attenuator shown in Fig. 9. With this circuit one can theoretically achieve any value of attenuation with a perfect match at the input and output ports provided that the series and shunt resistors, R_1 and R_2 , respectively, are given by

$$R_1 = Z_0 \left[\frac{K^2 - 1}{2K} \right] \quad (4.5)$$

$$R_2 = Z_0 \left[\frac{K + 1}{K - 1} \right] \quad (4.6)$$

where

$$K = 10^{A/20} \quad (4.7)$$

A is the attenuation (in dB), and Z_0 the characteristic impedance of the transmission line connecting the input and output ports. Table 2 illustrates

18-6-20669

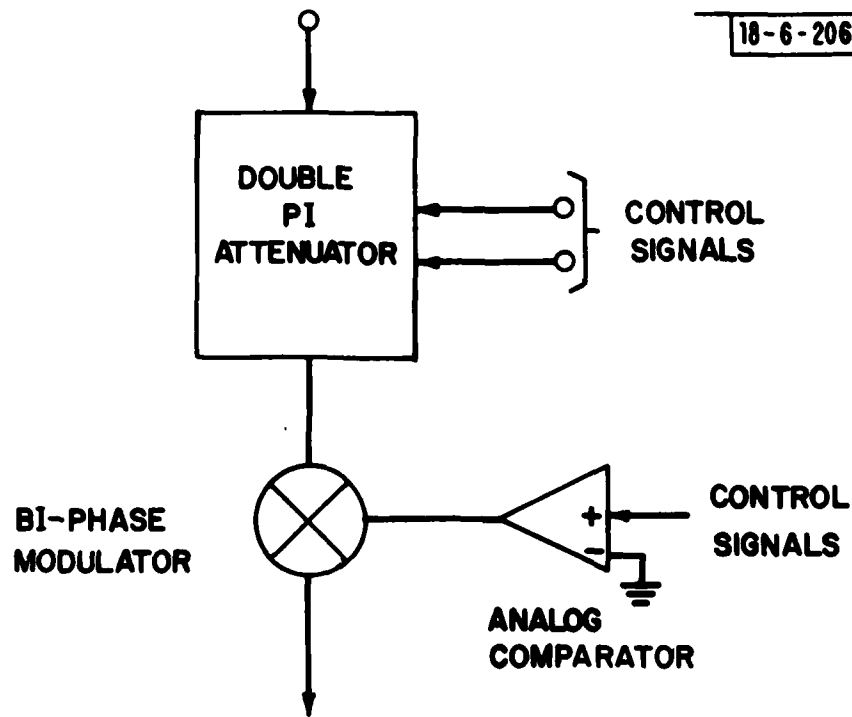


Fig. 8. Broadband attenuator/modulator circuit consisting of a double pi attenuator and a double balanced mixer operated as a biphasic modulator.

18-6-20670

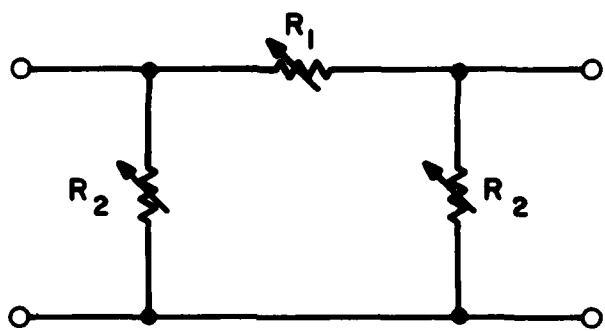


Fig. 9. Variable resistance pi attenuator circuit.

the values of the series and shunt resistances required at various attenuation settings over a 40 dB dynamic range. It can be noticed that as the attenuation becomes small the series resistance approaches zero ohms as expected, and the shunt resistance approaches infinity. At the other extreme, when large attenuations are needed, the series resistance approaches infinity and the shunt resistance approaches z_0 .

TABLE 2
SERIES AND SHUNT RESISTANCE VALUES FOR A
PI-ATTENUATOR CIRCUIT vs ATTENUATION
($z_0 = 50$ ohms)

<u>Attenuation (dB)</u>	<u>R₁ (ohms)</u>	<u>R₂ (ohms)</u>
0	0	∞
1	2.5	2000.4
10	71.1	96.3
20	247.5	61.1
30	790.0	53.3
40	2500.0	51.0

When PIN diodes are used as the elements in a variable pi attenuator, the minimum attenuation is generally limited to roughly 1 dB due to the large bias currents required to achieve the small resistance in the series diode. The maximum attenuation, on the other hand, is determined by the extent to which the series diode can be turned "off". Unfortunately, as the series diode is turned "off", its junction capacitance becomes an important component in the diode impedance, and the resulting parallel RC network formed by the diode resistance and the parallel junction capacitance introduces a phase shift which varies with attenuation. For small values of attenuation (< 20 dB)

the change in phase with attenuation is generally quite small, but increases rapidly with attenuation and can approach 80° or more for a 40 dB attenuation change. One method for minimizing this phase change is to use two attenuator sections cascaded together where each attenuator is operated over one-half the total attenuation range.

Fig. 10 illustrates the schematic diagram of the double pi attenuator used in the broadband weight circuits. The attenuator consists of two pi sections cascaded together, and is designed to operate with two bias signals, one variable for controlling the attenuation and one fixed for obtaining the impedance match at the input and output ports. The PIN diodes, represented by D1, D1', D2, D2' and D3, assume the role of the series and shunt resistors in a conventional pi attenuator. However, instead of using three diodes for each attenuator section for a total of six diodes, the circuit in Fig. 10 is configured so that D3 is shared between the two pi sections. The remaining resistors and capacitors form the impedance matching and diode biasing circuits.

To understand the operation of the circuit in Fig. 10 let us assume for the moment that a fixed negative voltage is applied to the fixed bias port, and the variable bias port is open circuited so that diodes D1 and D1' are "off". This condition corresponds to maximum attenuation since the series diode impedance is at its maximum value; this condition also leads to maximum phase shift (and hence maximum dispersion) as described previously, so that in practice the maximum attenuation must be limited, to 50 dB or less, by preventing D1 and D1' from completely turning "off". Obtaining the proper impedance match at the input and output ports requires that the input impedance at each port be approximately 50 ohms (assuming $Z_0 = 50$ ohms). This is achieved by applying a negative voltage at the fixed bias port, and selecting the values of R1, R1', R2, R2', R3 and R4 so that diodes D2, D2' and D3 conduct to produce an effective input and output impedance of Z_0 . As the voltage at the variable bias port is made negative, diodes D1 and D1' begin to conduct currents, I_c and I_c' , through the dc circuit formed by R1, D1 and R5, and R1', D1' and R5', respectively. This current flow causes the impedance of D1 and D1' to become smaller which,

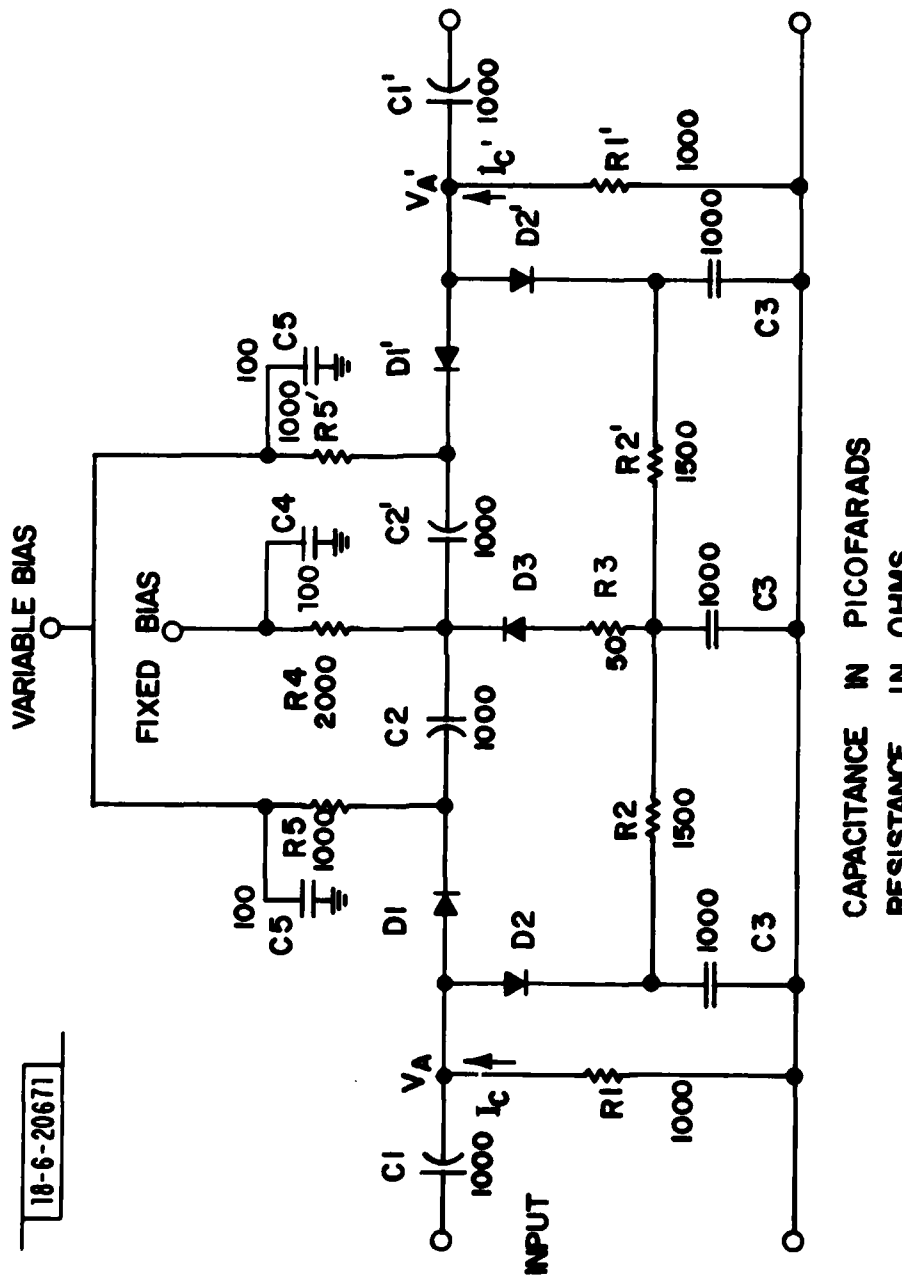


Fig. 10. Schematic diagram of the double pi attenuator circuit used in the broadband PIN diode weight circuit.

in turn, reduces the circuit attenuation. Correspondingly, as I_c and I_c' increase, the voltage across the input and output resistors, V_a and V_a' , becomes more negative which causes less current flow through D2, D2' and D3. With these diodes now conducting less current, their impedance increases, thereby producing a larger shunt resistance across the circuit at the input and output ports. As the attenuation is reduced further, the voltage drop across R1 and R1', due to the large currents through D1 and D1', will eventually approach, or exceed the fixed bias voltage, so that no current will flow through D2, D2' and D3. In this state, D2, D2' and D3 are "off" and the shunt circuit impedance is at its maximum value. Therefore, with the proper selection of the bias resistors, the fixed bias voltage and the diode resistance vs current characteristics, one can control the variation of the shunt impedance so that the impedances at the input and output ports are reasonably well matched to the transmission line over the full attenuation range. The component values shown in Fig. 10 are those values which give the best overall circuit performance as determined from measurements and computer simulations of the circuit

Because of the large number of different components used in the broadband weight circuit, it was decided to fabricate the RF circuit using microwave hybrid integrated techniques as a means for reducing the circuit size and for minimizing circuit parasitics. Each double pi attenuator circuit was fabricated on a separate one-inch square alumina substrate, 0.025-inch thick, using gold metalization, thin-film ceramic chip resistors, low loss miniature porcelain ceramic chip capacitors, and chip PIN diodes. The individual components were attached to the substrate using either gold epoxy or gold bonding wires. The quadrature hybrid power divider used at the input of the weight circuit was attached to a second one-inch square substrate while a third substrate, 1 x 2 inches, was used for mounting the two biphase modulators and output power combiner. Fig. 11 illustrates a completed RF weight module showing the interconnection of the various substrates, the input/output RF connectors, and the weight control inputs. To complete the assembly of the broadband weight circuit, the RF weight module was connected to a second module

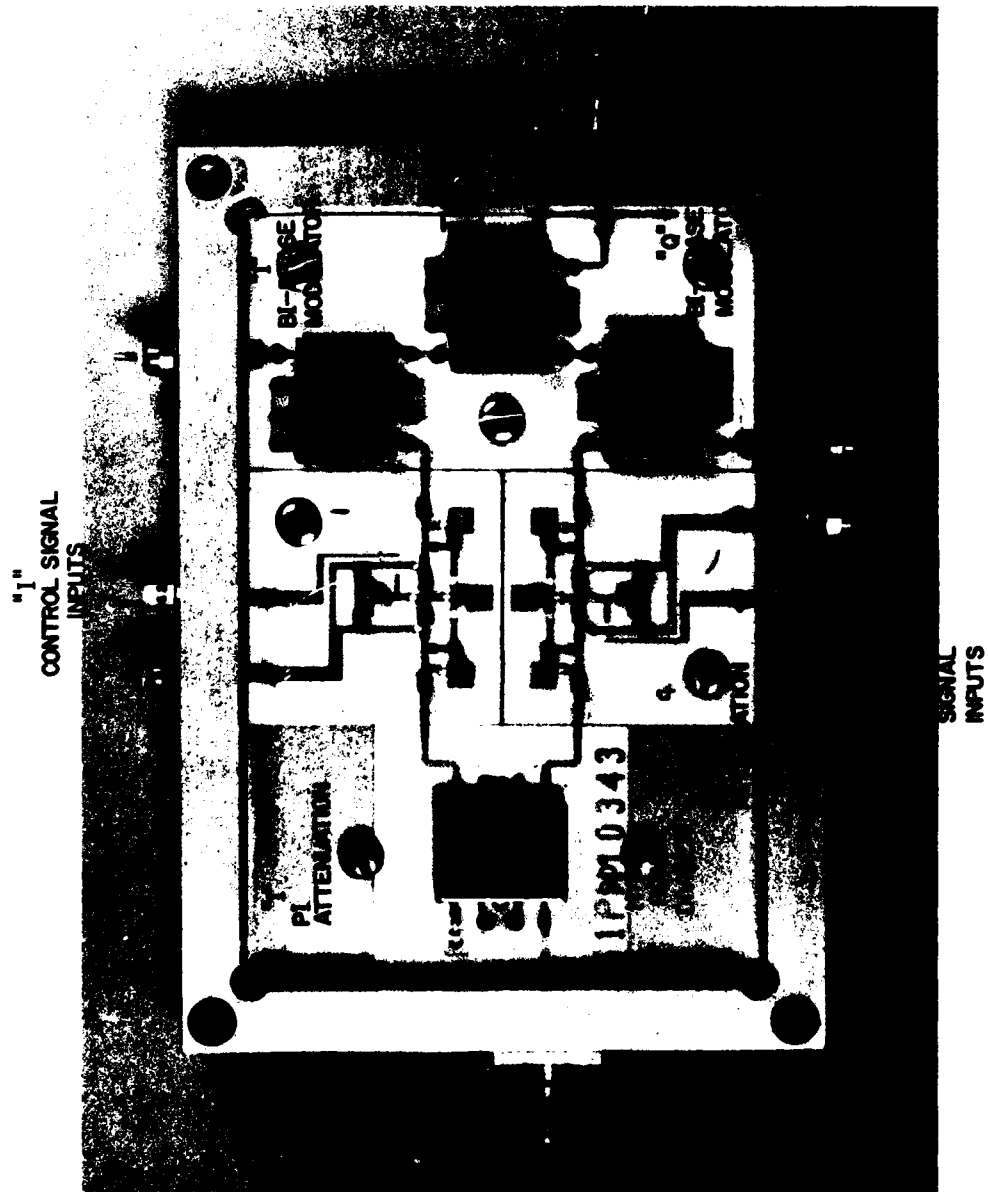


Fig. 11. Broadband RF weight module.

containing a two-way power divider, and both modules were mounted on a flat plate containing the weight driver electronics. Photographs of a complete weight assembly are illustrated in Fig. 12 and Fig. 13.

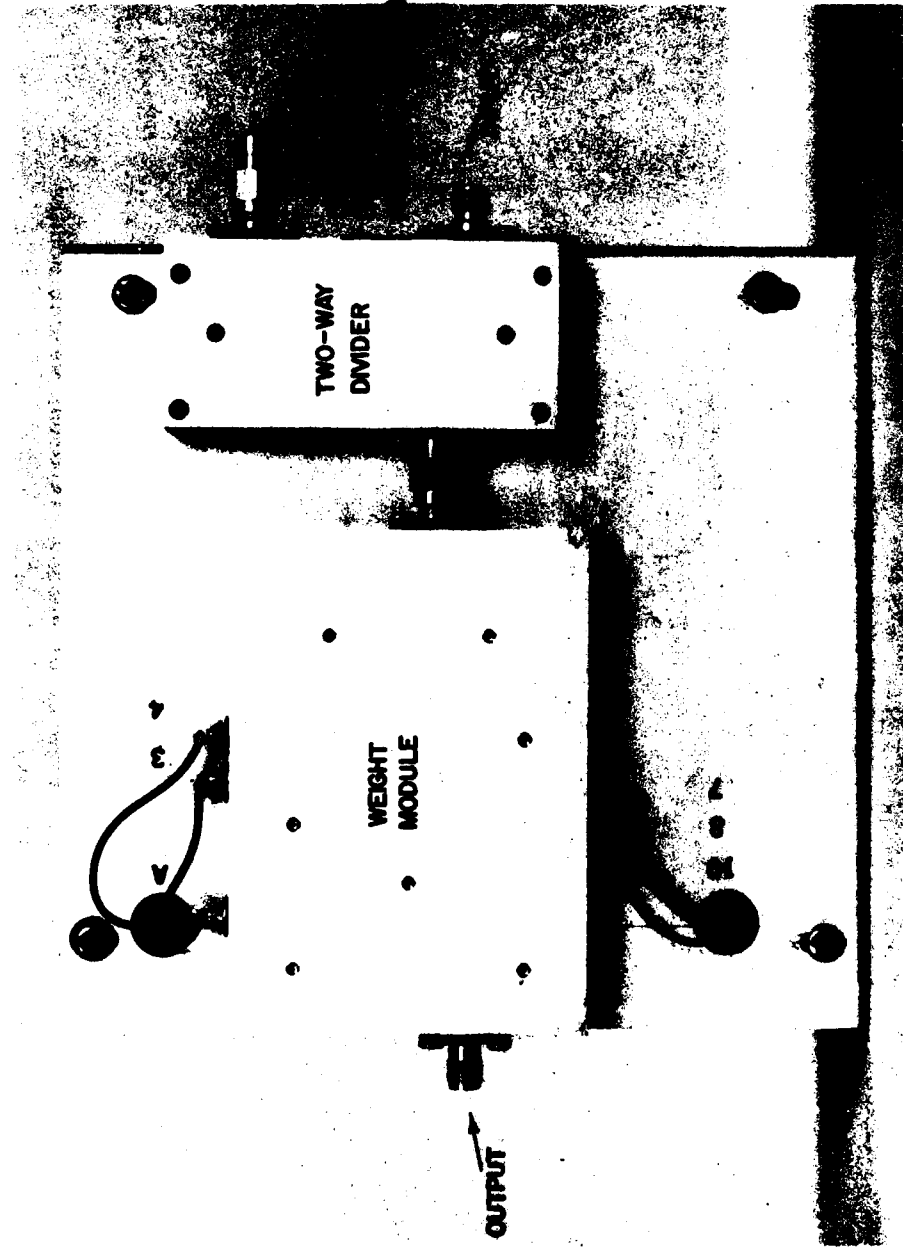


Fig. 12. Front side view of broadband PIN diode weight circuit showing RF weight module and two-way divider.

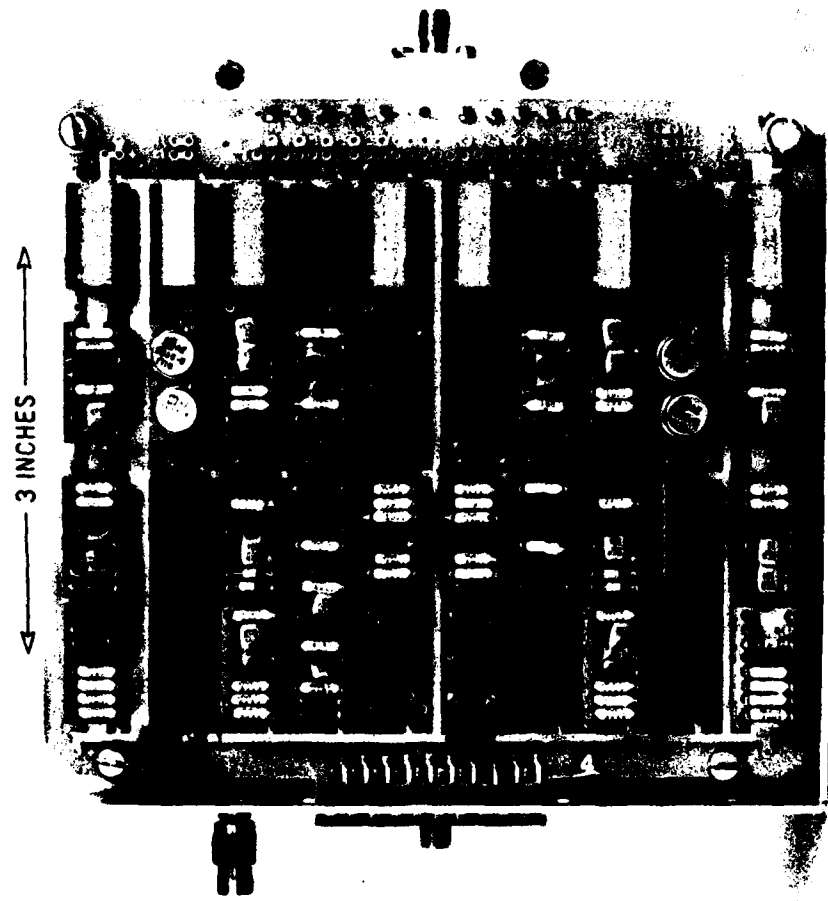


Fig. 13. Rear side view of broadband PIN diode weight module showing driver circuit.

CP202-2913

V. SINGLE WEIGHT PERFORMANCE

5.1 Narrowband Weight Circuits

Initial testing of the narrowband weight circuits was concerned with evaluating the performance of the "I" and "Q" attenuator/biphase modulator circuits, followed by measurements on a complete weight circuit. The measured performance of a typical circuit showing the attenuation and phase of the output signal as a function of control voltage is shown in Fig. 14 for control voltages over the range from ± 1 volt (0 dB) to ± 0.003 volt (50 dB). From Fig. 14 the following observations can be made:

1. The relative attenuation is linear with control voltage (to within ± 1 dB) over approximately 30 dB.
2. The dynamic range of attenuation is limited to approximately 35 dB.
3. Insertion phase is relatively constant for small attenuations (< 10 dB) but increases rapidly at higher attenuation levels.

Increasing the dynamic range significantly beyond 35 dB is very difficult with this circuit design because of the limitations in fabricating hybrid power dividers with isolation levels higher than about 35 dB over the full 10 MHz IF bandwidth. Also, for a large dynamic range it becomes increasingly more difficult to select pairs of diodes whose resistances track sufficiently well. To achieve 40 dB of attenuation, for example, requires that both diodes be set within 0.5 ohm of 50 ohms (simultaneously) over the IF band. As a means for determining diodes best suited for this application, measurements were made on several diodes from different manufacturers, in various configurations (ceramic "pill" packages and axial lead glass encapsulated diodes) with carrier lifetimes ranging from 0.1 μ sec to 2 μ sec. Final selection was based on resistance tracking characteristics and intermodulation performance. After considerable testing, the diode selected was an axial lead, glass encapsulated PIN diode (GHz Devices Model 4433) having a 2 μ sec lifetime.

The choice of diode lifetime was dictated largely by the intermodulation (IM) performance and the fact that higher levels of intermodulation were

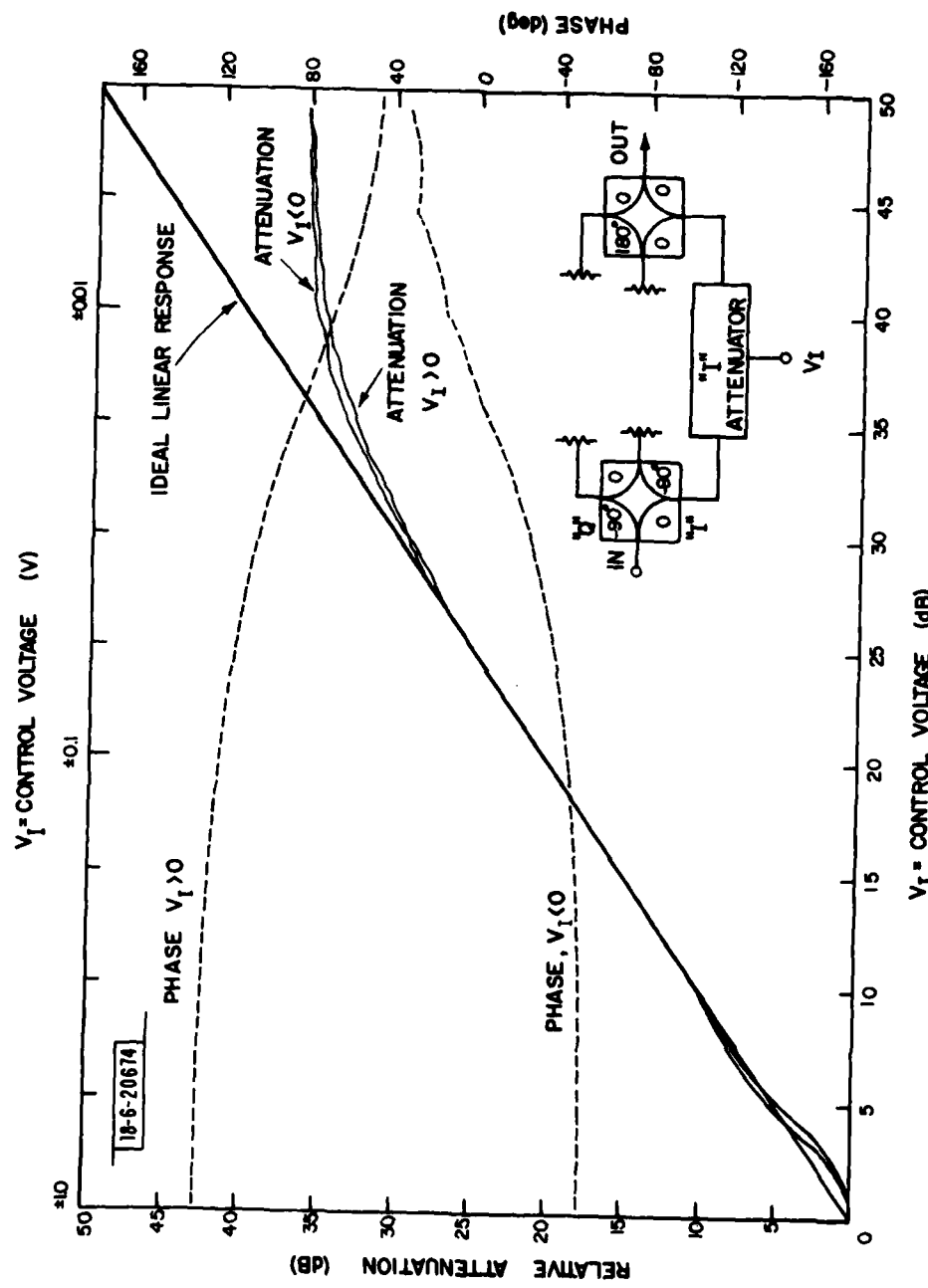


Fig. 14. Attenuation and phase response of the "I" channel of weight #2 vs control voltage, V_I , at 12.5 MHz.

observed in diodes having lifetimes less than 1 μ sec. Since the diode lifetime is a measure of the time required for stored charge in the I region to be depleted by recombination once the forward bias is removed, it cannot be chosen too large so as to limit the diode response time. That is, for a maximum IF bandwidth of, say, 500 KHz, the diode should be capable of responding in 2 μ sec or less, and as a rule of thumb, diodes having lifetimes of 2 μ sec or less would satisfy this requirement.

Intermodulation measurements were made by inputting two equal amplitude cw tones (at -10 dBm) separated in frequency by 20 KHz (121.87 and 121.89 MHz) and measuring the two tone and third order IM products at the output using a spectrum analyzer (the fifth and higher order products were found to be negligible). Tests conducted on the attenuator circuits using different diodes have shown that in all cases the intermodulation level increases with attenuation, reaching a maximum level when the circuit attenuation is approximately at its maximum value; that is, when both PIN diodes are biased near 50 ohms and are absorbing maximum RF power. However, there was a significant difference noted in the IM level which depended upon the diode lifetime. For an attenuator circuit using 0.1 μ sec lifetime diodes biased for approximately 30 dB attenuation, the third order IM level was -52 dBm, 12 dB below the -40 dBm tone outputs. In order to satisfy the intermodulation specification (see Table 1), it was necessary to use diodes with a 2 μ sec lifetime (GHz Devices Model 4433). Using these diodes, the third order intercept exceeded +15 dBm at minimum attenuation and at 30 dB attenuation, the IM level was -75 dBm, or 35 dB below the two-tone output level.

IM measurements were also conducted on the full weight circuits to assess their performance as a function of weight setting. The measurements, in this case, were conducted as before except that one of the attenuator circuits was left full-on (i.e., at maximum attenuation) while the other attenuator was varied over its full range. Fig. 15 illustrates the signal levels at the output of the weight circuit as a function of the relative weight setting. The

18-6-20675

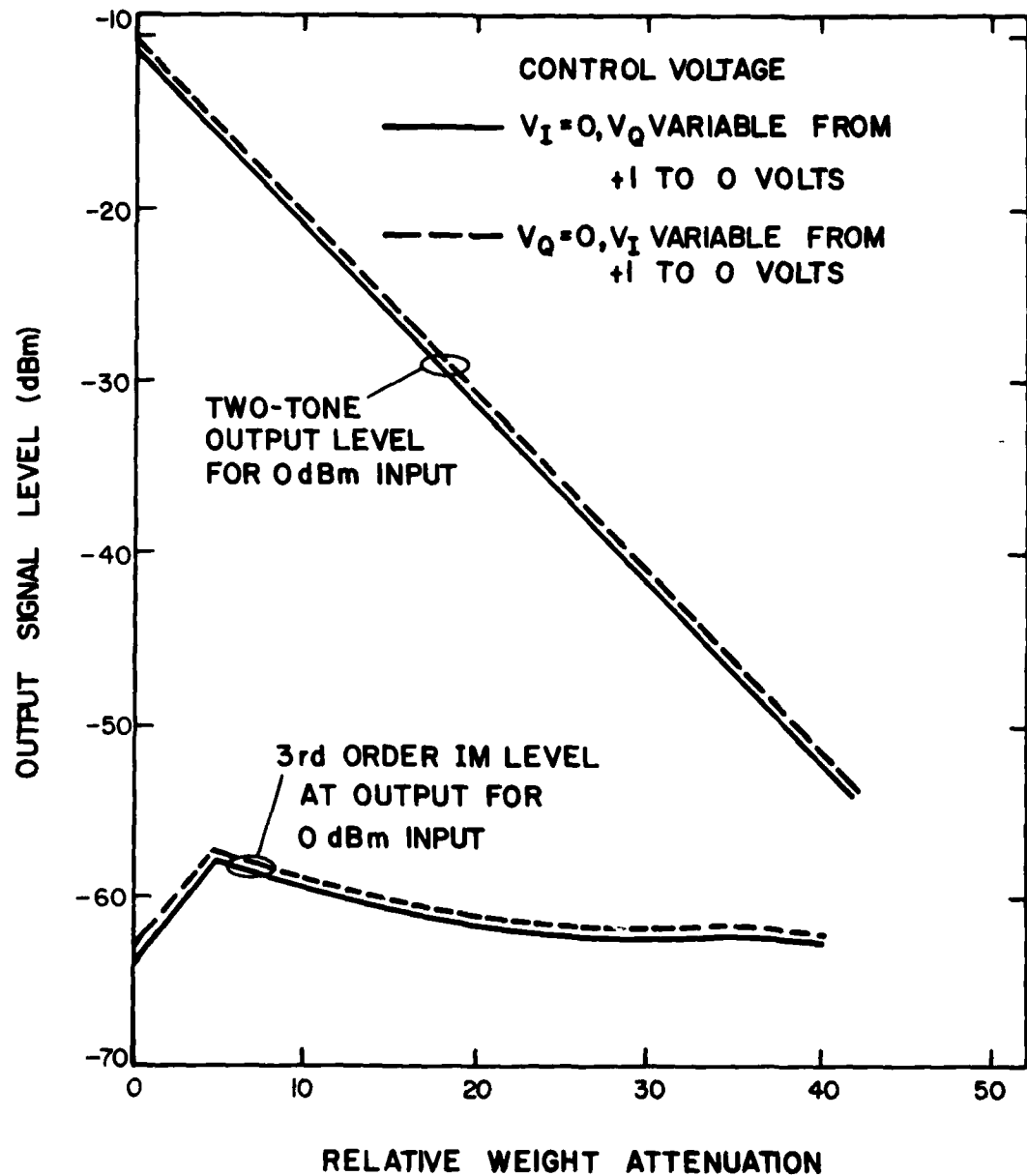


Fig. 15. Intermodulation measurements for narrowband weight circuit.

data presented here represents the worst case performance since one of the attenuators is always set for maximum attenuation, a condition which produces maximum IM level. Under these conditions the IM level is essentially constant over the full range of weight attenuation, at a level of approximately -62 dBm when two 0 dBm input tones are applied at the input*.

Fig. 15 also illustrates that a full weight circuit can achieve an attenuation which is larger than that obtained with either the "I" or "Q" attenuator circuits (typically 35 dB). This occurs because, at a fixed frequency, the weighted output signal can be adjusted so as to cancel any non-weighted (i.e., feed-through) signals which occur at the output. Thus, at a single frequency, a very large value of attenuation can be produced. However, over a frequency band the maximum attenuation can vary widely depending upon the level of the feed-through signal and the time delay difference between the weighted and non-weighted signal component (See Eq. 4.3). Fig. 16 illustrates a typical response of a single weight circuit versus frequency when the weight has been adjusted for maximum attenuation at the IF center frequency (121.4 MHz). It can be observed that the attenuation increases rapidly with frequency away from the center frequency and that over the 10 MHz bandwidth the maximum attenuation remains below 45 dB**.

* Since the weight circuit and the two-way divider circuit preceding the weight circuit are contained on the same RF microstrip circuit (see Fig. 6), the input signal level at the two-way divider input is 0 dBm, and approximately -3 dBm into the weight circuit.

** It should be noted that 45 dB is the minimum value of maximum attenuation over a 10 MHz band when the weight is adjusted to form a null at the IF center frequency. Operating the weight in this fashion is permissible when the phase of the weight is not important, such as when a channel is being turned off. However, the maximum weight which can be achieved for an arbitrary phase setting is determined by the dynamic range of the attenuator circuit which, in this case, is approximately 35 dB.

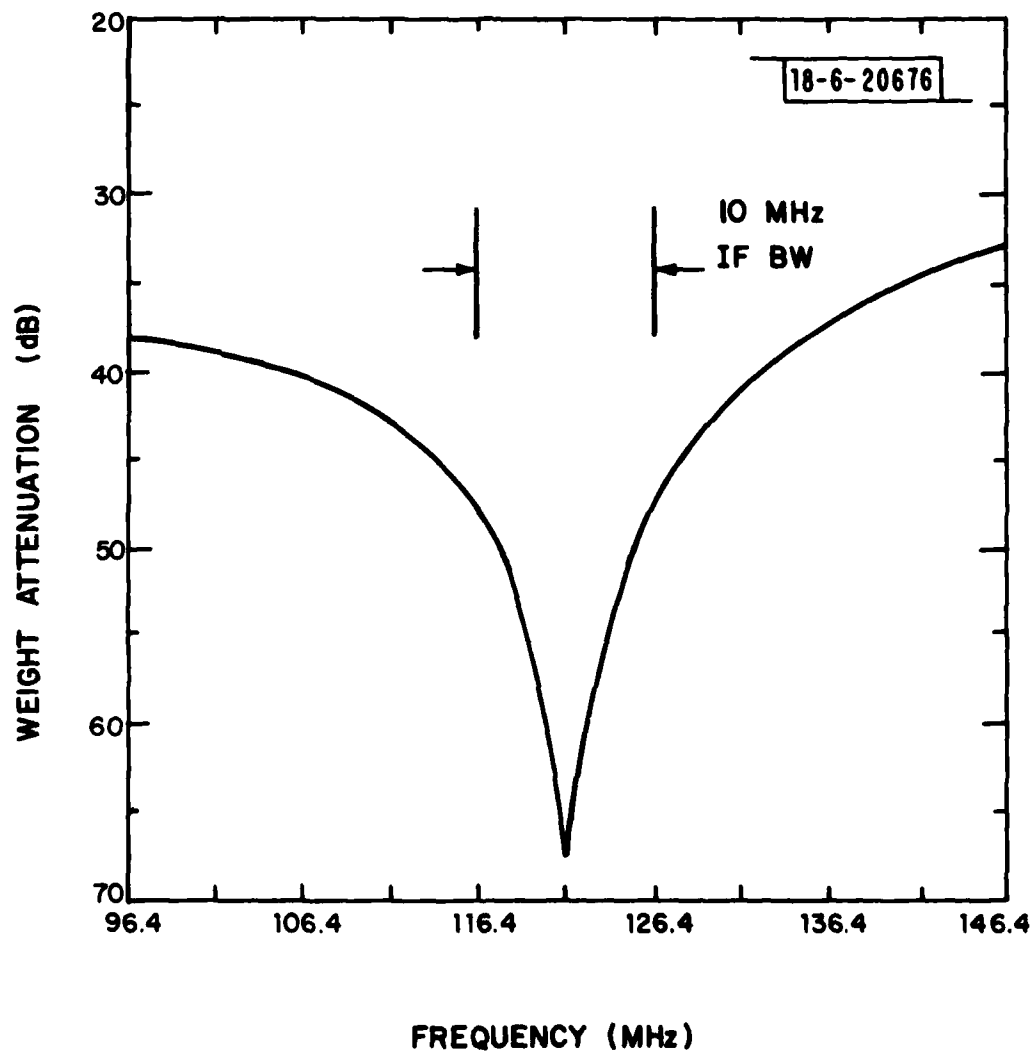


Fig. 16. Weight attenuation vs frequency obtained by adjusting weight for maximum attenuation and sweeping frequency.

The presence of non-weighted feed-through signals at the output of the weight circuit was found to be highly detrimental to the tracking performance, and in fact, the major factor limiting the performance of the weight circuits. Although spurious signals are present at the output of any weight circuit, those occurring at the output of the narrowband weights are particularly a problem because they tend to be correlated from weight to weight. As a result of this coherence, the spurious output signals tend to add vectorially resulting in an output signal level which increases as N^2 (assuming equal feed-through levels), as indicated in Eqn. 4.4, where N is the number of weight circuits. Thus when the tracking performance of two weights is measured and characterized, the equivalent performance for eight similar weight circuits could be a factor of sixteen worse (12 dB). Because of the importance of channel matching on the processor performance, extensive testing was done to characterize the tracking performance of the weight circuits. These measurements are presented later, in Section 6.

5.2 Broadband Weight Circuits

The overall performance of the broadband weight circuits was found to be substantially better than that achieved with the narrowband weight circuit. A large part of this is due to improvements made in the design and fabrication of the weight attenuator circuit. Since each attenuator is mounted on a separate substrate, each circuit was tested individually and the driver circuit adjusted to optimize the insertion loss, return loss and linearity of the attenuator prior to installation into the weight module. This resulted in a substantial improvement in the overall weight performance.

Figure 17 illustrates the typical performance characteristics of the double pi attenuator. It is capable of achieving a dynamic range of 50 to 60 dB with a linearity of approximately ± 2 dB over the full range, a phase shift with attenuation of less than 20 degrees over a 40 dB range, and a return loss which averages 15 to 20 dB (VSWR < 1.3). Over the 10 MHz IF bandwidth the attenuation and phase shift were essentially constant, varying

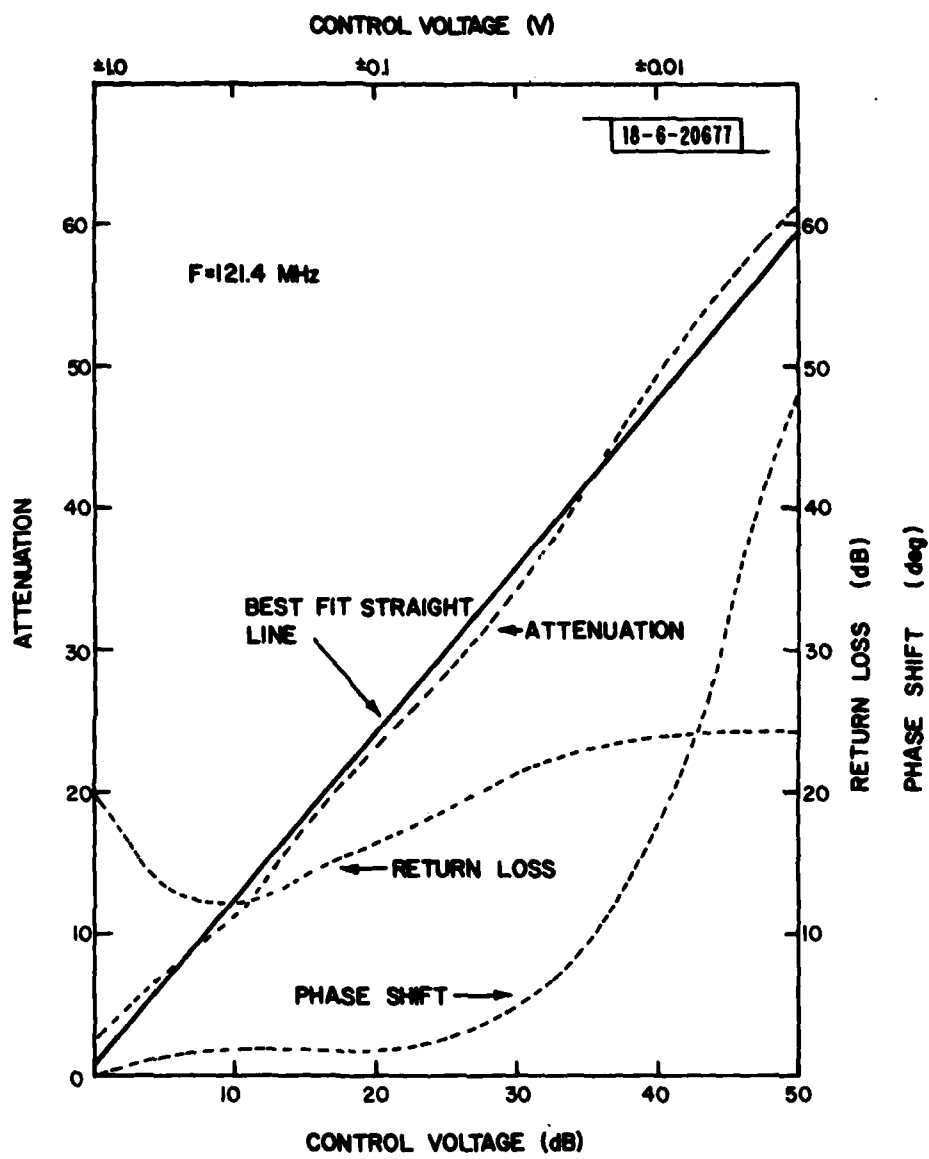


Fig. 17. Attenuation, return loss and phase shift as a function of control voltage at 121.4 MHz for a double pi attenuator circuit.

less than ± 0.05 dB at 40 dB and $\pm 0.9^\circ$ (worst case), respectively. Measured results showing the attenuation for several values of control voltage are plotted in Figure 18 as a function of frequency over a 500 MHz bandwidth.

As with the narrowband attenuator circuit, a series of measurements was conducted to determine the IM performance of the double pi attenuator and the weight circuits; these results are presented in Figures 19 and 20, respectively. The data in both figures were obtained by applying two 0 dBm* cw tones at the input and measuring at the output the two tone and IM levels. For both circuits, the IM level was found to be acceptable and considerably lower than those measured in the narrowband weight circuit. The IM performance of the attenuator circuit (i.e., the IM level vs attenuation) was found to be essentially independent of the input level when measured at +10 dBm and -10 dBm (except of course for the characteristic 3 dB/dB change in the absolute IM level). That is to say, the third order two tone intercept point, when referred to the output, was found to be constant (+23 dBm at 0 dB attenuation) for input levels less than +10 dBm (no measurements were made above +10 dBm). The weight modules, on the other hand, were observed to have a third order intercept point which is lower for +10 dBm input tones than that obtained with 0 dBm input tones (4 dBm vs 15 dBm at 0 dB attenuation, respectively). This increase in IM level is apparently the result of additional IM signals being generated by the biphasic modulator circuit (the double balanced mixer) when it is operated near its compression point (specified as 0 dBm into mixer). Although operating the weight circuit at higher input levels** represents some degradation in IM performance, this was not felt to be a problem since the IM signals at the output are always at least 40 dB below the two tone level over the full attenuation range.

* For the weight modules, which were tested after final assembly, the input signals were not applied directly to the weight input but to the two-way divider circuit in front of the weight circuit (see Fig. 12).

** The highest input signal to the weight circuit when installed in the processor is less than +7 dBm.

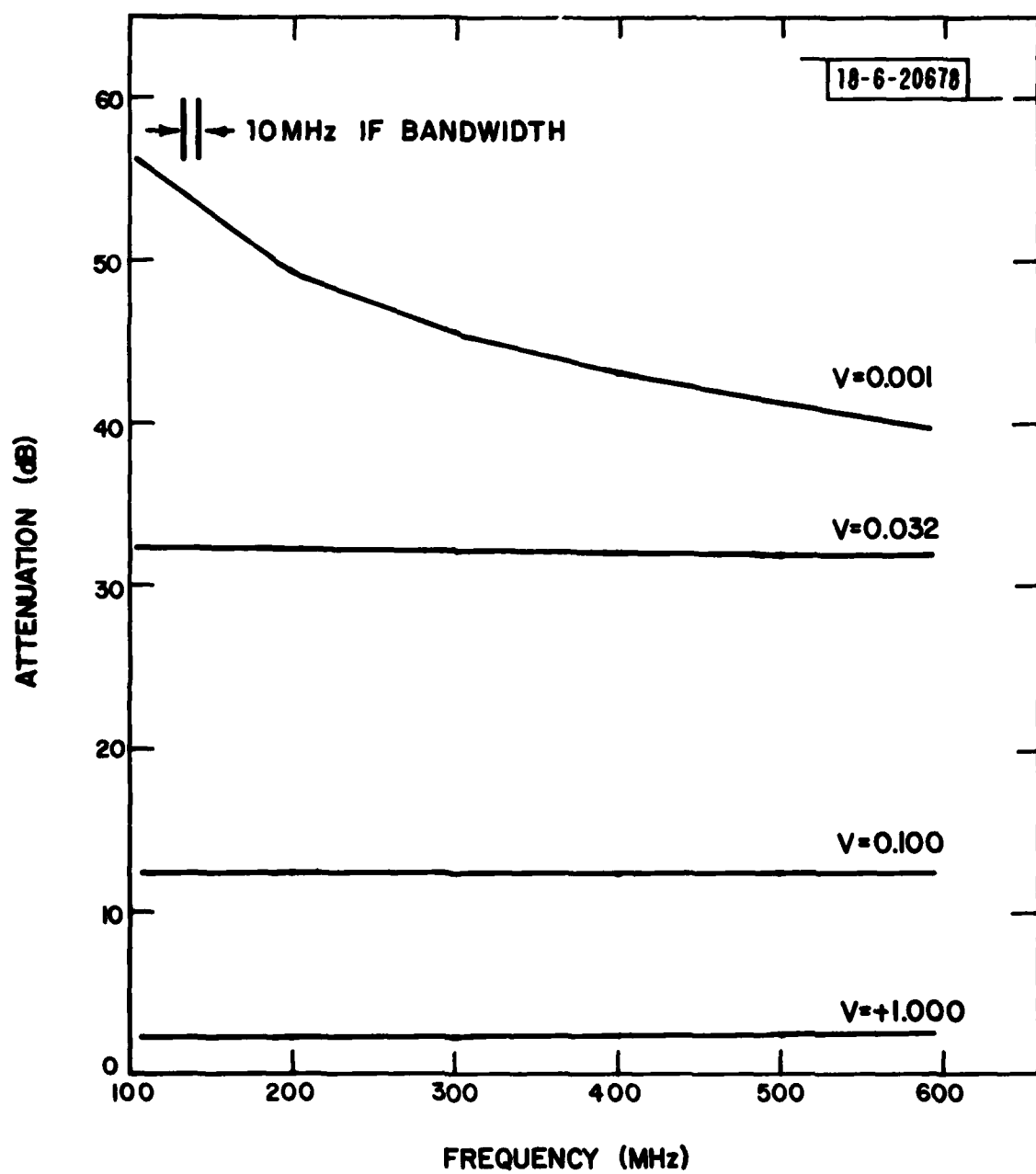


Fig. 18. Attenuation vs frequency for double pi attenuator for variable control voltages.

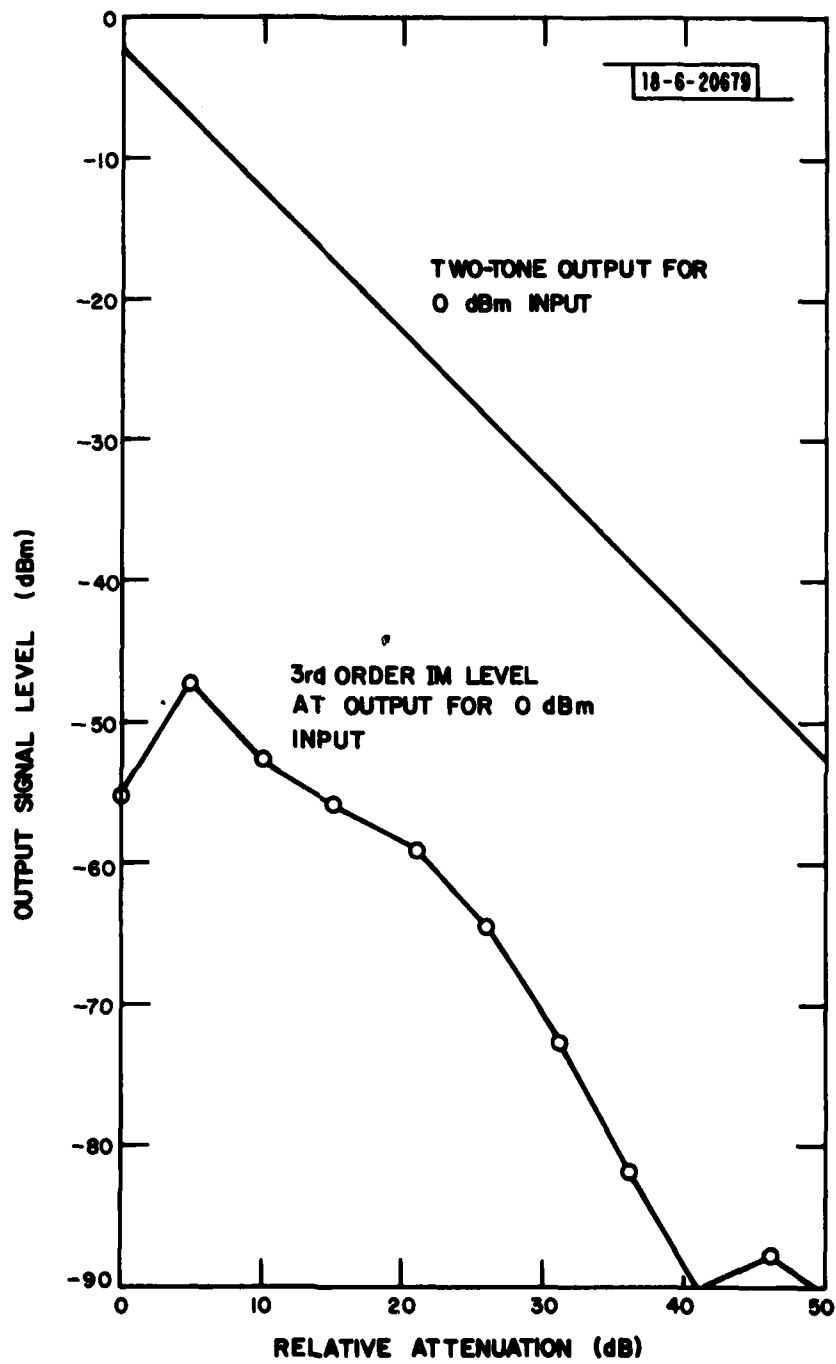


Fig. 19. Intermodulation performance vs attenuation for double pi attenuator.

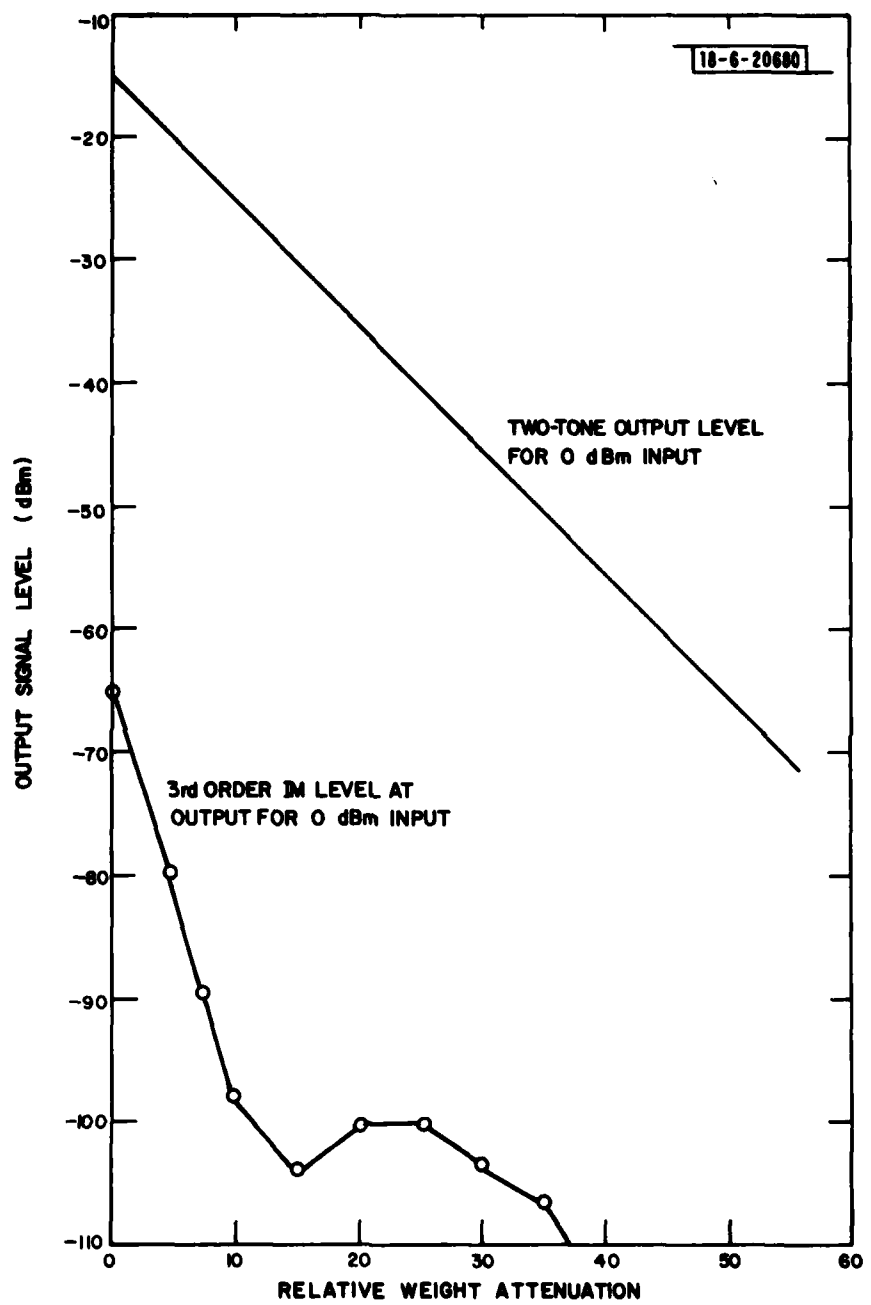


Fig. 20. Intermodulation vs attenuation for broadband weight circuit.

VI. WEIGHT TRACKING PERFORMANCE

6.1 Measurement Techniques

The basic measurement system used in characterizing the weight tracking performance is shown in Fig. 21. It consists of an RF source, a programmable switch network, a network analyzer for measuring amplitude and phase, D/A converters for activating the switch relays and for generating the weight control signals, and a programmable desk top calculator for automating the measurement and data collection functions. The switching network is comprised of a set of single-pole-double-throw (SPDT) switches, connected between a 4-way divider/combiner network, which terminate all channels into matched loads when not in use. With the switch network it is possible to connect various numbers of weight circuits (up to four) between the combiner/divider thereby allowing measurements to be made on single weights, any combination of two weights, etc., up to four weights. For the measurement of single weights, the switch network can be removed and the weights measured directly by connecting them, one at a time, between the source and network analyzer. This modification eliminates the insertion loss and tracking errors associated with the switch network, and improves the overall measurement accuracy.

One obvious requirement of the measurement system in Fig. 21 is that the switch network must have tracking errors which are much smaller than those of the weighting circuits which are being evaluated. Therefore, during the design and fabrication of the switch network considerable effort was devoted to measuring and adjusting the various channel transfer functions to be the same. By carefully selecting components and trimming each channel (using shunt reactive and resistive components) to modify its amplitude and phase response, it was possible to achieve a rms channel mismatch difference of less than 0.01 dB and 0.1 degree over a 50 MHz measurement band, corresponding to an effective cancellation level of approximately -55 dB (see Fig. 2).

Before discussing the measurement results let us first briefly describe the two measurement techniques used to evaluate the weight tracking performance. In the first method, the weight tracking performance was deduced by connecting

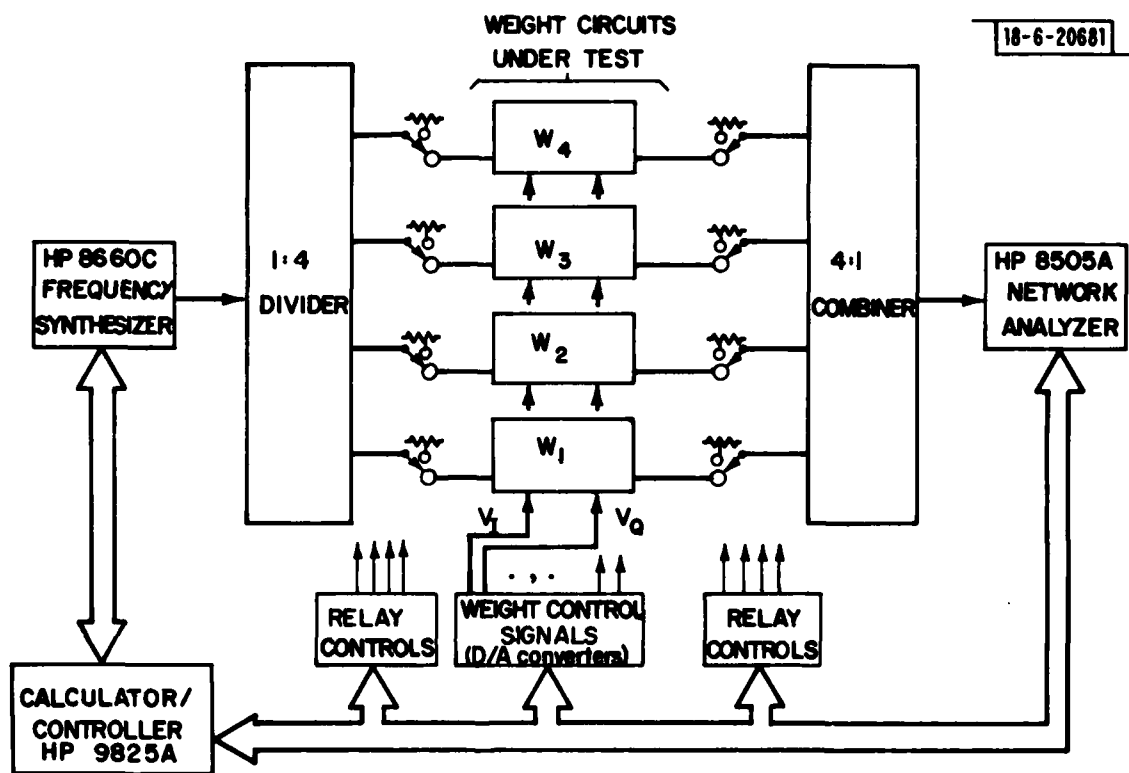


Fig. 21. Automated test set-up for characterizing weight tracking performance.

several weights in parallel as shown in Fig. 21, inputting a cw signal (at band center) to the switch network and adjusting the weight control voltages (closed loop) so as to null the output signal. Once the weights have adapted to null the output signal, the weight control voltages are fixed and the input signal frequency is varied across the measurement band. The variation in the output power versus frequency is a direct result of differences in the frequency response functions of the weight circuits, and in fact, can be shown to be related to achievable cancellation level^[8]. More will be said about this later.

In order to drive the weights closed loop so as to null the output, all that is required is a set of D/A converters for generating the weight control voltages and a digital algorithm for controlling the weights. For an Applebaum-Howells adaptive loop of the type used in the adaptive processor, each weight circuit satisfies a first-order differential equation of the form^[1],

$$\tau \dot{W}_k + W_k + \mu C_k = B_k \quad , \quad k = 1, 2, \dots, N \quad (6.1)$$

where $W_k(t)$ = complex weight for k -th channel

$\dot{W}_k(t)$ = dW_k/dt

τ = closed loop time constant

μ = feedback loop gain

$C_k(t)$ = complex output of correlator

B_k = complex steering signal specifying the quiescent weight setting obtained when no sources of interference are present (i.e., the unadapted weight setting)

Using the above notation the processor output, $V_o(t)$, becomes

$$V_o(t) = \sum_{\substack{\text{All} \\ \text{Channels}}} w_k(t) E_k(t) \quad (6.2)$$

and $C_k(t)$ can be expressed as

$$C_k(t) = E_k(t) V_o^*(t) \quad (6.3)$$

where $E_k(t)$ is the complex signal into the weight circuit, and "*" indicates a complex conjugate.

To obtain a discrete time (recursive) solution to Eq. (6.1) suitable for implementation with the digital controller in Fig. 21, we make the following assumptions and definitions:

1. Assume the input to the switch network is a cw tone at the center of the band ($\omega = \omega_0$), and denote the result of the nth iteration on the variables as $V_o(\omega_0, n)$ and $C_k(\omega_0, n)$ where $\omega_0 = 2\pi f_0$ is the cw tone input frequency.
2. Assume that each weight can be characterized approximately as a linear function of its control voltage so that,

$$w_k = v_k = v_{k,I} + jv_{k,Q}$$

where $v_{k,I}$ and $v_{k,Q}$ are the real and imaginary components of the k-th weight control voltage.

3. Approximate $\tau \dot{w}_k$ as

$$\tau \dot{w}_k = \tau \dot{v}_k = \frac{1}{\epsilon} [v_k(n+1) - v_k(n)]$$

where $n = 1, 2, \dots, M$ is the iteration number

$$V_k(n+1) = (n+1) - st \text{ estimate of } V_k$$

$$\epsilon = \text{iteration step size } \sim \mu/10$$

4. With each weight initially in its full on position (i.e., minimum attenuation with $V_{I,k} = 1, V_{Q,k} = 0$), switch between channels and sample each channel in amplitude and phase. Denote this result as $X_k(\omega_0, 0)$.

5. Define the equivalent correlator output for the recursive solution as

$$C_k(\omega_0, n) = X_k(\omega_0, 0) V_o^*(\omega_0, n)$$

Substituting (1) - (5) into Eq. (6.1) and noting that for $n=1$, $B_k = V_k(1)$, we obtain a set of recursive equations in terms of the complex weight control voltages,

$$V_k(n+1) = (1-\epsilon) V_k(n) - \mu \epsilon X_k(\omega_0, 0) V_o^*(\omega_0, n) + \epsilon V_k(1), \quad n=1, 2, \dots, M \quad (6.4)$$

where $V_o(\omega_0, n)$ is the measured output of the switch network for the n -th iteration and M is the total number of iterations. After the above iteration converges (as determined by measuring the output power), the weight control voltages are fixed, and the output power is measured vs frequency. The ratio of the average output power over the measurement band before and after convergence is a measure of the cancellation obtained with the weight circuit and is given by

$$C = \frac{1}{T} \sum_{j=1}^T |v_o(\omega_j, n)|^2 / \left(\frac{1}{T} \sum_{j=1}^T |v_o(\omega_j, 1)|^2 \right) \quad (6.5)$$

where T is the total number of frequencies at which measurements are made.

In order to use Eq. (6.4) to drive the weights closed-loop, one must first specify the initial conditions defining the steering voltages, $v_k(1)$, the loop gain parameter, μ , and the iteration step size, ϵ . As an example of how these parameters might be chosen, let only a single weight be "on" in the unadapted state, so that the steering vector is $B^+ = [0, 1, 0, 0]$ where the "1" appears in the reference (or "on") channel. (Which channel we choose as the reference channel is not arbitrary, however, as it has been shown that choosing a dominant error channel as reference degrades the performance significantly^[8]. In fact, if one measures the nulled output power vs frequency for various selections of reference channels, there will be one channel which yields the best cancellation. Thus a typical measurement scenario might consist of measuring the nulled output power obtained when each of the weights is selected as a reference.) The selection of μ determines the extent to which the output power level is reduced, and therefore should be chosen large enough to characterize the weight performance over a large dynamic range. It was found that for most measurements choosing a value of 10^4 for μ was adequate since this value will allow 80 dB of cancellation (theoretically) for zero bandwidth (i.e., cw tone input). ϵ , on the other hand, represents the iteration increment and must be small enough to ensure convergence but yet large enough to obtain convergence with a reasonable number of iterations; values ranging from $1/2 \mu$ to $1/10 \mu$ were found to be adequate for most measurements.

When selecting the D/A converters in Fig. 21, one must be careful to use a sufficient number of bits to provide the resolution and accuracy needed for setting the weight control voltages. For example, over the ± 1 volt range of control voltage, 60 dB attenuation requires a control voltage of 1 millivolt (assuming an ideal, linear weight) and a D/A converter having at least 12 bits.

The second method for characterizing weight tracking performance is based on a statistical analysis of the measured weight transfer functions. Each weight circuit is measured by connecting it directly between the source and network analyzer and measuring its transfer function for a selected control voltage setting. From these data, estimates can be obtained of the weight

tracking errors and of the corresponding cancellation performance. Unlike the previous method which computes the cancellation in terms of the nulled output power versus frequency, in this method the cancellation performance is determined by detecting very small differences in the transfer function data. Consequently, the measurement system must be calibrated very carefully to ensure the accuracy of the measurement data. The measurement system in Fig. 21 uses a state-of-the-art network analyzer which incorporates a vector error correction capability (in software) for enhancing the measurement accuracy. With this system, accuracies of 0.01 dB and 0.1 degree are achievable, corresponding to cancellation levels of ~ -55 dB.

The procedure for determining cancellation using this method can be described as follows. Let us define $W_k(\omega)$ as the weight transfer functions obtained as a function of frequency when each weight is measured for some specific control voltage. The set of data corresponding to $W_k(\omega)$ is processed by estimating the $N \times N$ average cross-correlation matrix between weight circuits according to

$$\underline{R} = \frac{1}{FBW} \int_{\frac{1-FBW}{2}}^{\frac{1+FBW}{2}} W_k(\omega') W_q^*(\omega') d\omega' \quad k, q = 1, 2, \dots, N \quad (6.6)$$

where $\omega = 2\pi f_0$ denotes the center frequency, $\omega' = \omega/\omega_0$, and FBW the fractional bandwidth about ω_0 . Corresponding to \underline{R} , one can define an eigenvalue equation,

$$\underline{R} \cdot \underline{e}_k = S_k \underline{e}_k \quad k = 1, 2, \dots, N \quad (6.7)$$

the solution of which defines a set of eigenvalues, S_k , and their associated eigenvectors, \underline{e}_k . Since the eigenvalues of \underline{R} can be computed for a fixed value of FBW, they can be considered as being a function of FBW. When $FBW \rightarrow 0$, \underline{R} will have only a single non-zero eigenvalue, S_1 , indicating that perfect cancellation can be obtained for a cw tone using only a single degree of freedom

corresponding to this eigenvalue. As FBW increases, differences in the frequency variations between weights then lead to other non-zero eigenvalues which characterize the tracking error.

A detailed discussion of the eigenvalue spectrum and its relationship to cancellation performance is presented in Ref. [9]; there it is shown that the dependence of cancellation on bandwidth can be determined directly from the eigenvalue spectrum when computed as a function of bandwidth. To characterize the weight tracking performance would require that the complex transfer function of each weight circuit be measured for a large number of weight settings. Not only would this require a considerable expenditure of time and effort, it would be very difficult, if not impossible, to measure the transfer functions to the required accuracy over the full range of weight settings. Alternately, one can measure the weight transfer functions for a few selected weight settings, and from these measurements use the eigenvalue spectrum to estimate the tracking performance. From the eigenvalue spectrum one can then estimate the upper bound on the cancellation performance from the ratio of the two largest eigenvalues of \underline{R} , i.e.,

$$C \leq K \frac{s_2}{s_1} \quad (6.8)$$

where K is a constant whose value depends upon the steering vector. For an N element processor, K generally varies from 1 to N depending upon the type of steering vector desired so that the upper bounds on the cancellation become

$$\begin{aligned} C &\leq N \frac{s_2}{s_1} && \text{(Single Non-zero Quiescent Weight)} \\ C &\leq \frac{s_1}{s_2} && \text{(All Quiescent Weights Non-zero)} \end{aligned} \quad (6.9)$$

To summarize, the procedure for determining the weight tracking performance from the eigenvalue spectrum is as follows. With a fixed I and Q weight control voltage (such as $V_I = 1$, $V_Q = 0$), the amplitude and phase response of each weight is measured as a function of frequency with a network analyzer. The

correlation matrix, \underline{R} , is computed from the data (using Eq. 6.6) parametrically as a function of the fractional bandwidth, FBW. The eigenvalues of \underline{R} are then computed (Eq. 6.7) and plotted as a function of FBW, from which an estimate of the cancellation (upper bound) can be obtained using Eq. (6.9).

6.2 Measurement Results

The digital feedback algorithm described in the previous section was used to evaluate the tracking performance of both the narrowband and broadband weight circuits. Fig. 22 illustrates the results obtained for a single narrowband weight circuit at $f_o = 121.4$ MHz for several selections of the loop parameters, μ and ϵ . Since the algorithm attempts to minimize the output power, the only way it can do this for a single weight is to maximize the weight attenuation by turning the weight off. The amount by which the weight is to be turned off, however, is determined by the loop gain parameter, μ , according to

$$\text{Max Attenuation} = 20 \log (\mu) \quad (6.10)$$

so that for the two values shown in Fig. 22, ($\mu = 10^2$ and 10^4) the maximum (theoretical) attenuation levels are 40 dB and 80 dB, respectively. As a practical matter, attenuation levels above about 60 dB are difficult to obtain (reliably) due to the quantization errors and noise associated with the D/A converters which are used to set the weight control voltages. At 60 dB the required control voltage setting is one millivolt (assuming an ideal linear weight), which is of the same order of magnitude as the noise level (specified as ± 0.2 millivolt peak-to-peak) and quantization errors (LSB = ± 0.5 millivolt) associated with the 12 bit D/A converters. For these reasons, the weight adaption is stopped once the attenuation reaches 65 dB.

When two or more weight circuits are tested closed-loop, the output power is minimized by adjusting the weight control voltages so that the weighted signals combine to form a null at the output. The final ideal adapted weight settings in this case are determined by the initial steering signals applied to

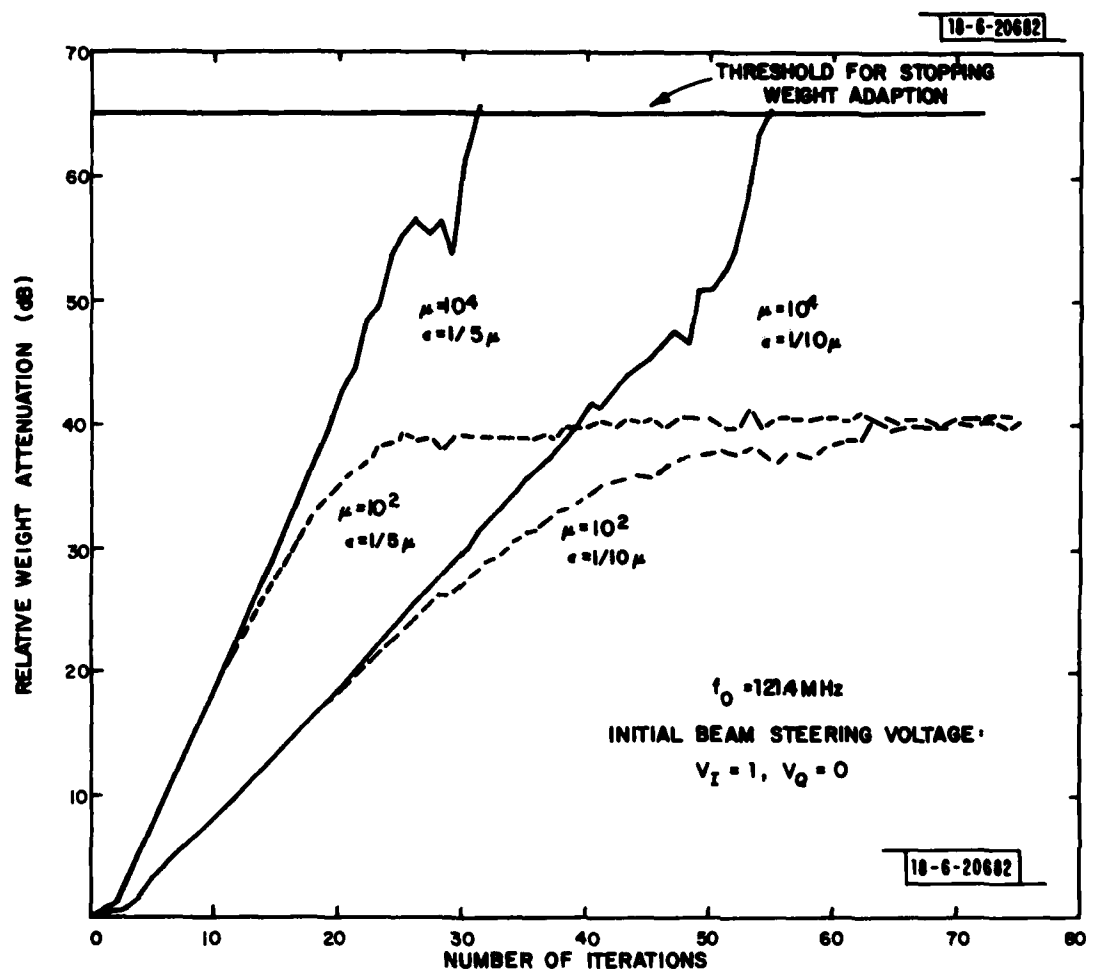


Fig. 22. Measurements conducted on a single narrowband weight circuit illustrating weight attenuation vs number of iterations for selected values of μ and ϵ .

the weights before the weight adaptation begins. As an example, consider a four-element system with only a single channel on; the beam steering vector for this case might be expressed as

$$\underline{B}^\dagger = [1, 0, 0, 0] \quad (6.11)$$

where the "1" is applied to the reference or "on" channel and the remaining weights are "off". The final ideal adapted weight settings for a cw source applied equally to all channels are given by

$$\underline{W}^\dagger = [\frac{3}{4}, -\frac{1}{4}, -\frac{1}{4}, -\frac{1}{4}] \quad (6.12)$$

indicating that the reference channel weight is set to 2.5 dB (and 0°) while the remaining weights each have 12 dB attenuation (at 180°). With these weight settings applied to each channel, perfect cancellation is obtained.

To illustrate the tracking performance of multiple weight circuits, Fig. 23 shows the cancellation in output power plotted as a function of frequency for the following three cases:

1. when a single narrowband weight is turned "off" with $B = 1$,
2. for two narrowband weights with $\underline{B}^\dagger = [1, 0]$, and
3. for four narrowband weights with $\underline{B}^\dagger = [1, 0, 0, 0]$

In each case the measurements were performed by selecting channel 1 as reference and allowing the weight circuit(s) to adapt at $f_o = 121.4$ MHz so as to null the output power. The weight control voltage settings are then fixed and the output power measured as a function of frequency. The rapid increase in output power at frequencies away from f_o is an indication of the dispersion between the feedthrough (non-weighted) signal component relative to the weighted output signal over the measurement band. It can also be observed that the output power level rises as more weights are added, increasing 4 to 6 dB as the number of weights are doubled. This N^2 dependence, where N is equal

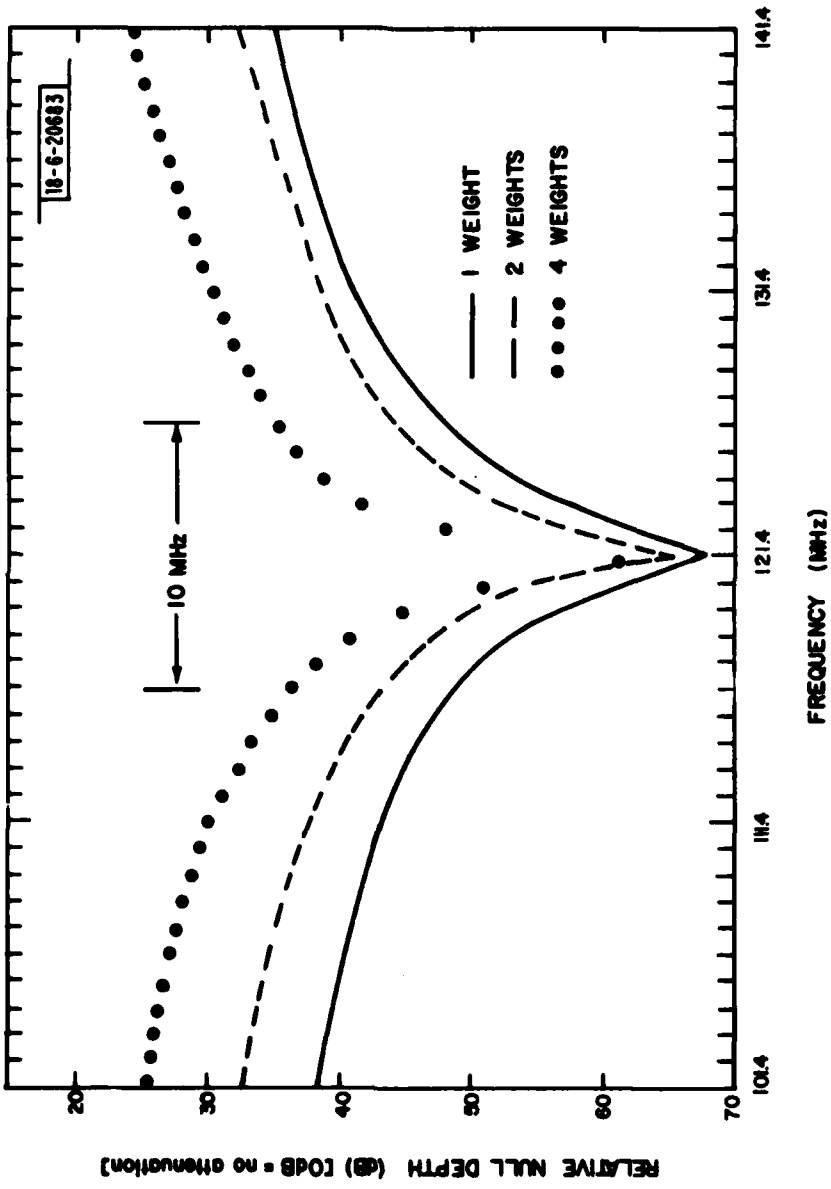


Fig. 23. Comparison of measured tracking data for narrowband weights showing null depth vs frequency for 1, 2 and 4 weights.

to the number of weights, is indicative of feed-through signals which are highly correlated from weight to weight. In fact, as indicated previously in Eqn. 4.4, correlated feed-through signals lead to a cancellation which varies as

$$C \leq N^2 |\gamma_o|^2 \frac{(\pi BW\tau)^2}{3} \quad (6.13)$$

Measurements similar to those shown in Fig. 23 were conducted on the broadband weight circuits to characterize their tracking performance. These results are presented in Fig. 24. Not only do the broadband weights provide a substantial reduction in the output level vs frequency, there also appears to be a smaller correlated feed-through component as evidenced by the small increase in output power in going from the two-weight to four-weight case. A more quantitative comparison of the tracking performance of the narrowband and broadband weight circuits can be obtained by computing the measured cancellation (using Eq. (6.5)). These results are presented in Table 3 and illustrate that a 15 to 20 dB improvement can be achieved with the broadband weights.

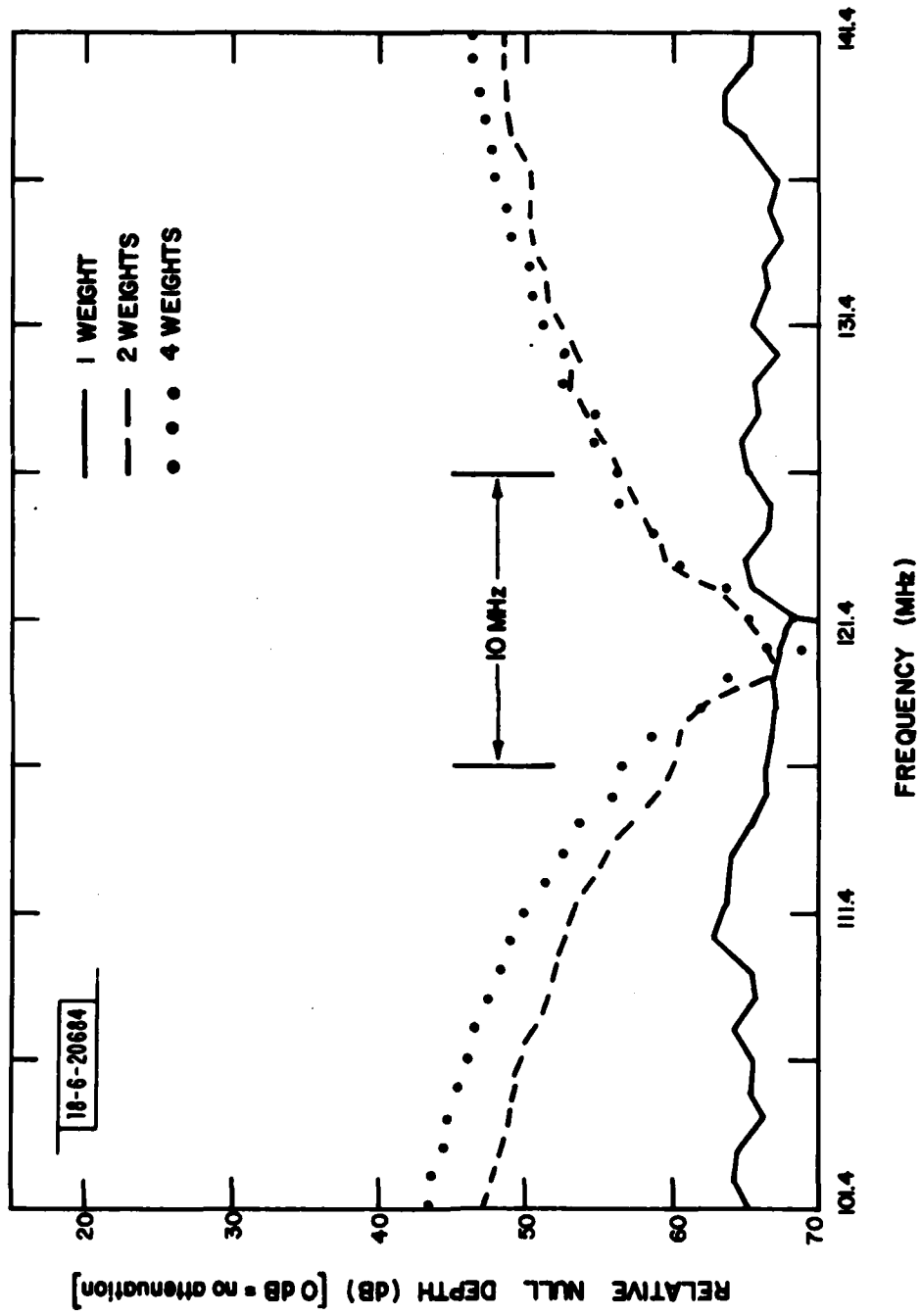


Fig. 24. Comparison of measured tracking data for broadband weights showing null depth vs frequency for 1, 2 and 4 weights.

TABLE 3
COMPARISON OF CANCELLATION OVER 10 MHz BANDWIDTH
AS A FUNCTION OF THE NUMBER OF WEIGHTS

	CANCELLATION (dB)		
	<u>N=1</u>	<u>N=2</u>	<u>N=4</u>
Narrowband Weights	-51.2	-46.7	-37.3
Broadband Weights	-66.5	-60.3	-59.1

Figs. 23 and 24 represent the weight tracking performance for a particular steering vector, choosing a specific weight as reference. To evaluate the tracking performance at other weight settings and for different selections of reference channels, one can imagine selecting the reference channel randomly and defining a random complex steering vector according to

$$|B_k| = \begin{cases} 1, & q=k \\ 0, & q \neq k \end{cases} \quad (6.14)$$

$$\text{Phase } B_k = -180^\circ \leq \xi \leq 180^\circ, \quad q=k \quad (6.15)$$

where q is the randomly selected reference channel and ξ a randomly chosen steering phase angle. Over a large number of such selections, one can then compute the statistics of the measured tracking performance and from this the cancellation performance. The cancellation performance obtained from a series of 40 separate measurements is presented in Fig. 25. In Fig. 25(a) the probability of exceeding a given cancellation is plotted as a function of the cancellation level with bandwidth as a parameter while Fig. 25(b) shows the cancellation vs bandwidth. These results correspond very closely to those presented previously for a single choice of steering voltage and reference channel. They indicate that over a 10 MHz band, there is an 80 percent probability of achieving a cancellation level of -55 dB.

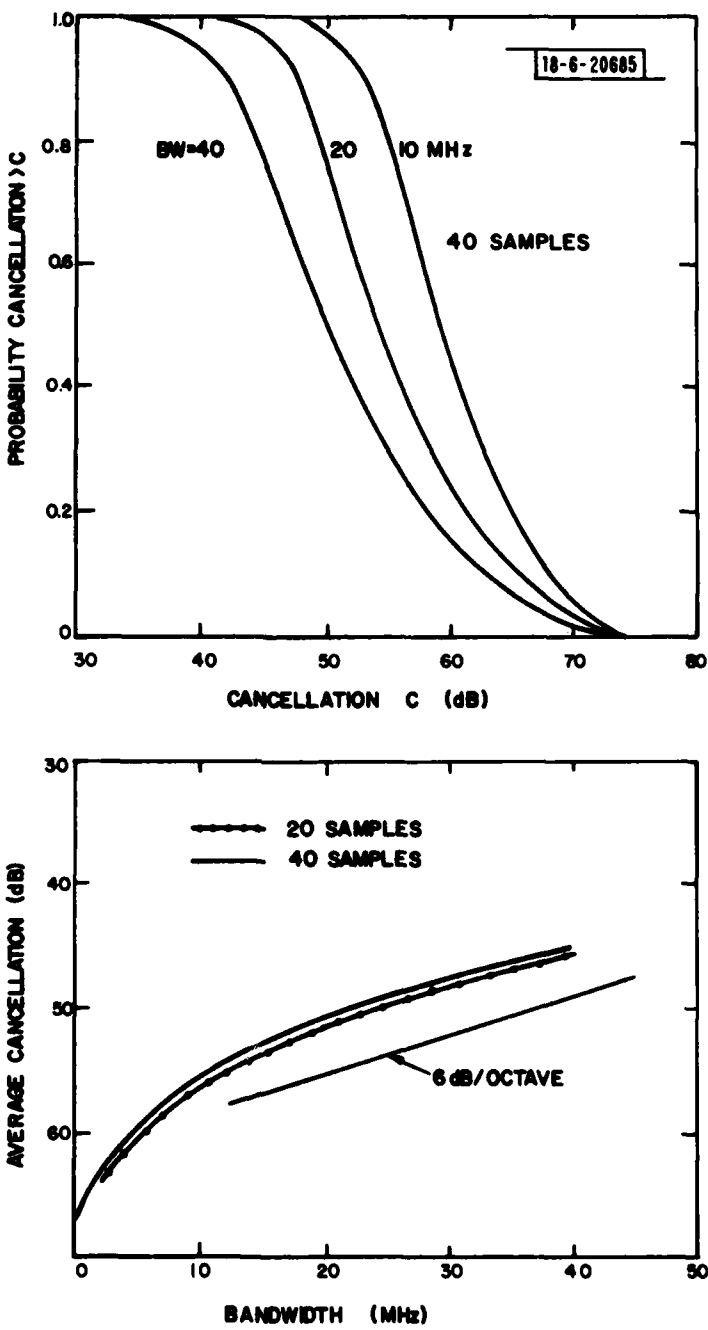


Fig. 25. Cancellation performance obtained from 40 random selections of the beam steering vector and reference channel.

The second method of determining tracking performance involved measuring the transfer function of each weight separately and computing the eigenvalue spectrum as described in the previous section. Fig. 26 illustrates the eigenvalue spectrum for the eight broadband weights computed from the measured correlation matrix as a function of bandwidth for a control voltage setting of $V_I = 0$, $V_Q = 1$. The dominant eigenvalue dispersion, s_2/s_1 is -53 dB at 10 MHz bandwidth which, from Eqn. 6.9, indicates that the cancellation upper bound is within the range of -44 to -53 dB. As bandwidth increases, s_2 and s_3^* are monotonically increasing functions of frequency indicating that a frequency dependence exists in the weights over large percentage IF bandwidths. For the narrowband weights this dependence is much more pronounced, with the levels of s_2 , s_3 , ..., s_8 being considerably higher.

Since the eigenvalue ratio, s_2/s_1 , is indicative of the cancellation performance which can be achieved using a single degree of freedom, it is instructive to compare the relative performance of the narrowband and broadband weights in terms of their s_2/s_1 ratios. Fig. 27 illustrates the spread in the eigenvalue ratio, s_2/s_1 for six different sets of control voltages. Over the 10 MHz IF bandwidth the broadband weights show a significant improvement (~ 15 dB) in the cancellation level in comparison to the narrowband weights.

One of the useful features of the eigenvalue plots presented in Figs. 26 and 27 is that they can frequently provide some insight into the nature of the mismatch errors. These particular figures show, for example, that for both sets of weights the eigenvalue ratio, s_2/s_1 , decreases approximately 6 dB for each octave increase in frequency. This suggests that the primary mechanism contributing to tracking errors has a bandwidth square dependence. One important class of errors exhibiting this type of behavior (i.e., $s_2/s_1 \sim BW^2$) are path length errors (i.e., time delay errors) which result in mismatch errors that are highly correlated from weight to weight. Errors of this type are present in almost any type of system requiring matched channels. They can occur, for example, because of small differences in electrical length between components, or due to impedance mismatches between components which give rise

* The higher order eigenvalues s_4 , s_5 , ..., s_8 are down -55 dB or less and below the measurement equipment sensitivity.

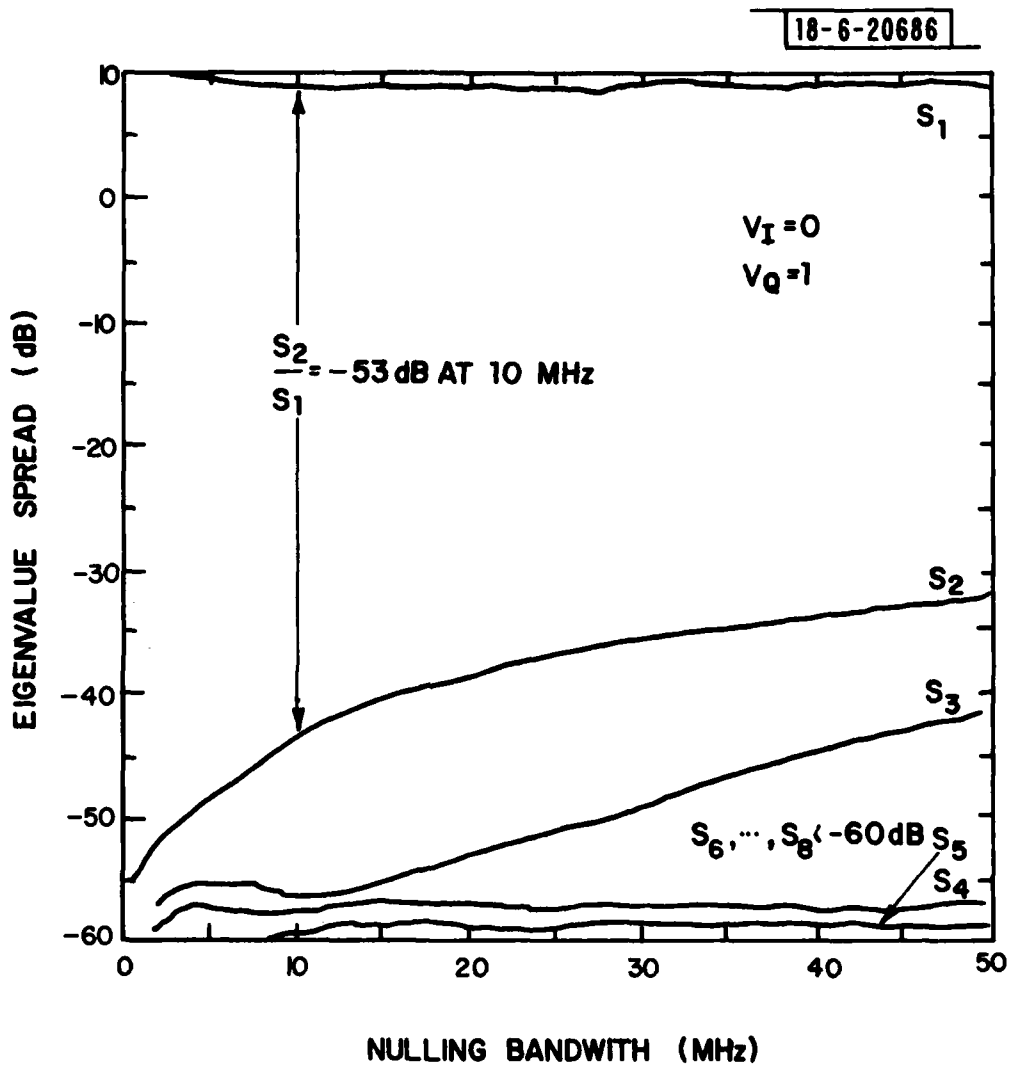


Fig. 26. Eigenvalues vs bandwidth for the eight broadband weight circuits, measured using a fixed control voltage $V_I = 0$, $V_Q = 1$ volt.

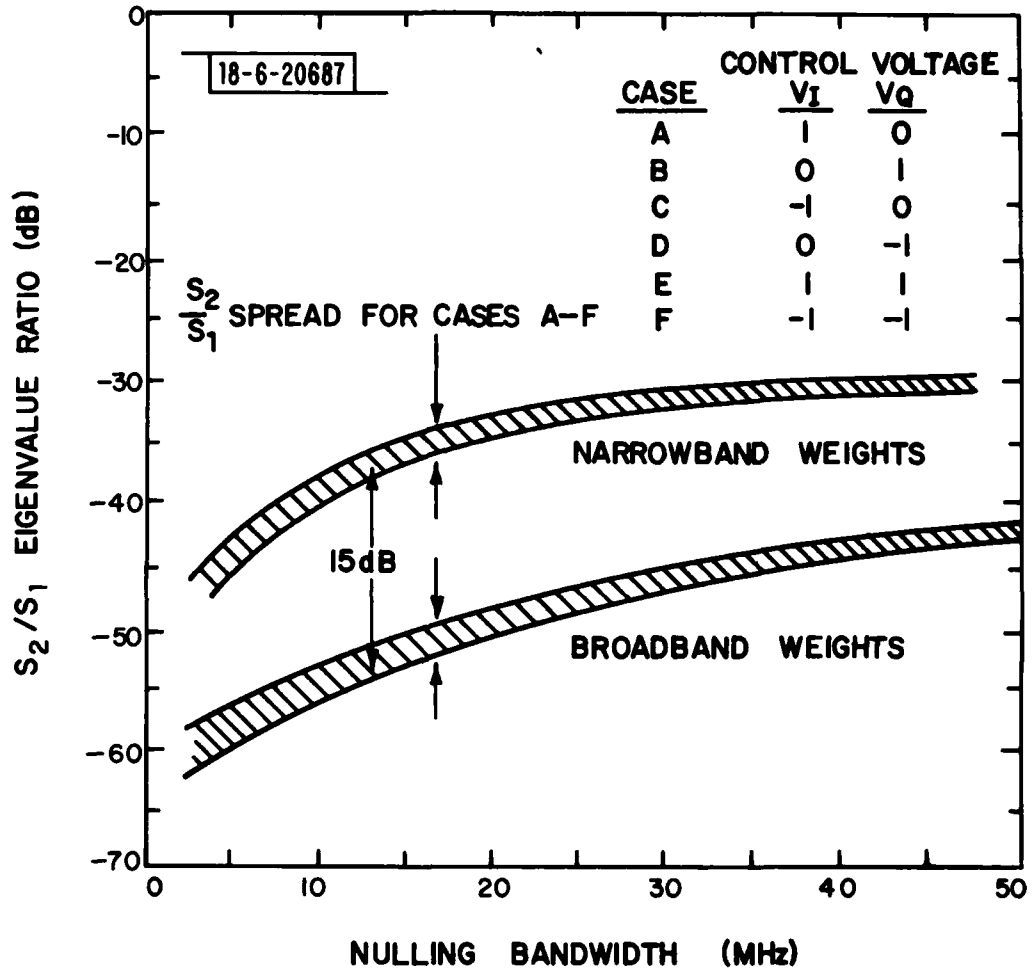


Fig. 27. Comparison of the eigenvalue ratio, s_2/s_1 , for the narrowband and broadband weights vs bandwidth.

to multiple reflections and hence, multiple time delays. For the narrowband weights, the primary factor limiting tracking performance was found to be due to a difference in time delay between the desired weighted signal, and undesired, feed-through signals occurring at the weight output as a result of the finite isolation of the weight attenuator circuits. The broadband weights, on the other hand, were found to have a tracking performance at least 15 dB better than the narrowband weight making it much more difficult to identify the mechanisms producing these spurious output signals. For these weights, the weight mismatch errors are most likely due to a combination of small time delay errors resulting from impedance mismatches, and low level "leakage" signals occurring at the output due to the finite dynamic range of the attenuator circuit.

VII. SUMMARY OF RESULTS

Table 4 presents a brief summary of the measured performance characteristics of the narrowband and broadband weight circuits. In comparison with the broadband weights, the narrowband weights were found to operate satisfactorily only over relatively small bandwidths (5 to 10%), with a tracking performance which is dominated by spurious signals (feed-through) at the weight output. The feed-through signals are the result of limitations in fabricating high input/output isolation quadrature hybrid power dividers which are used in the attenuator circuits. The 30 to 40 dB level of isolation achieved over the 10 MHz IF bandwidth resulted in a dynamic range of approximately 35 dB and severely limits the cancellation-bandwidth performance. The broadband weights, by comparison, have a minimum usable dynamic range of 50 dB, and a cancellation-bandwidth performance at least 20 dB better than the narrowband circuits.

The performance characteristics of the broadband weight circuits are of particular interest because of their potential use at higher RF frequencies. Operation at frequencies of several gigahertz should be possible with only minor modifications to the present circuit configuration.

Although neither weight was designed to minimize insertion loss, there are several areas where improvements can be made, particularly for the broadband weights, to reduce insertion loss. Modifying the drive circuit of the broadband weights to increase the bias current in the pi attenuator circuit would reduce its insertion loss to roughly 1.25 dB from its present value of 3 dB. Replacing the diode mixer in the biphase modulator with a lower loss design (e.g., a 90° hybrid with PIN diodes) would not only reduce the insertion loss (~ 1.5 dB), but should also improve the output impedance match and intermodulation performance.

TABLE 4

**COMPARISON OF PIN DIODE WEIGHT CIRCUIT PERFORMANCE
OVER 10 MHz IF BANDWIDTH CENTERED AT 121.4 MHz**

	<u>Narrowband</u>	<u>Broadband</u>
Insertion Loss ($V_I=1$, $V_Q=0$)	< 8.5 dB	< 12.4 dB
Input VSWR	< 1.2	< 1.2
Output VSWR	< 1.5	< 1.7
Dynamic Range (CW)		
Open Loop ($V_I=V_Q=0$)	35 dB typ.	> 50 dB typ.
Closed Loop	> 60 dB	> 70 dB
Single Weight Cancellation over BW ⁽¹⁾	45 dB typ.	65 dB typ.
Input Level for +1 dB Compression	> +10 dBm	+6 dBm ⁽²⁾
Two-Tone Third Order IM Intercept (referred to output) at Minimum Attenuation ($V_I=1$, $V_Q=0$)	+15 dBm min.	+14 dBm min.
Phase Variation vs Attenuation		
0 to 10 dB	2°	1°
0 to 20 dB	7°	2°
0 to 30 dB	22°	6°
Tracking Performance over 10 MHz BW (s_2/s_1 ratio)	-40 dB	-55 dB

(1) Relative to 0 dB at $V_I=1$, $V_Q=0$.

(2) Limited by the compression point of the double balanced mixer (i.e., the biphasic modulator)

ACKNOWLEDGMENTS

It is a pleasure to acknowledge the help and support of the many people who have contributed to the development of the PIN diode weight circuits. The author wishes to acknowledge the many helpful discussions with Dr. Joseph T. Mayhan, particularly with regard to the measurement techniques used in characterizing weight tracking performance. Special thanks are due to Larry Mandeville, Don Newcomb, and Reuben Patton for the many hours spent in fabricating and measuring the weight circuits; to Madhu Singhal for her programming support; and to John Milne, Peter Daniels, Doris Klays and Bill Fielding for their assistance in the fabrication of the broadband weight modules.

REFERENCES

1. W. F. Gabriel, "Adaptive Arrays - An Introduction," Proc. IEEE 64, 239 (1976).
2. D. A. Siegel et al., "Feedback Nulling Demonstration System Hardware," Technical Note 1979-12, Lincoln Laboratory, M.I.T. (23 November 1979).
3. J. T. Mayhan et al., "Feedback Processor Test Results," Lincoln Laboratory, M.I.T. Technical Note (to be published).
4. J. T. Mayhan, F. W. Floyd, "Factors Affecting the Performance of Adaptive Antenna Systems and Some Evaluation Techniques," Technical Note 1979-14, Lincoln Laboratory, M.I.T. (9 August 1979).
5. J. T. Mayhan, F. W. Floyd, "Some Effects of Hard Limiting in Adaptive Antenna Systems," Technical Note 1979-15, Lincoln Laboratory, M.I.T. (1 October 1979).
6. D. M. Hodson, "RF Front-ends for Feedback Nuller," Lincoln Laboratory, M.I.T. Technical Note (to be published).
7. J. N. Wright, "Transconductance Multipliers for Weight Circuits in an Adaptive Nulling System," Technical Note 1979-11, Lincoln Laboratory, M.I.T. (1 June 1979).
8. W. C. Cummings et al., "A UHF Test Simulator for an Antenna Nulling System," Technical Note 1979-8, Lincoln Laboratory, M.I.T. (7 June 1979).
9. J. T. Mayhan, "Bandwidth Limitations on Achievable Cancellation for Adaptive Nulling Systems," Technical Note 1978-1, Lincoln Laboratory, M.I.T. (17 February 1978), DDC AD-A054160.
10. D. M. Hodson, Lincoln Laboratory, M.I.T., private communication.

UNCLASSIFIED

SECURITY CLASSIFICATION OF THIS PAGE (When Data Entered)

19 REPORT DOCUMENTATION PAGE		READ INSTRUCTIONS BEFORE COMPLETING FORM	
1. REPORT NUMBER 18 ESD TR-79-306		2. GOVT ACCESSION NO. AD-A083 992	
4. TITLE (and Subtitle) 6 PIN Diode Weight Circuits ,		3. RECIPIENT'S CATALOG NUMBER	
7. AUTHOR(s) 10 Bing M. Potts		5. TYPE OF REPORT & PERIOD COVERED 9 Technical Note	
8. CONTRACT OR GRANT NUMBER(s) 14 TN-1979-26		6. PERFORMING ORG. REPORT NUMBER Technical Note 1979-26	
9. PERFORMING ORGANIZATION NAME AND ADDRESS Lincoln Laboratory, M.I.T. P.O. Box 73 Lexington, MA 02173		10. PROGRAM ELEMENT, PROJECT, TASK AREA & WORK UNIT NUMBERS Program Element No. 63431F Project No. 2029 15 F19628-80-C-0002	
11. CONTROLLING OFFICE NAME AND ADDRESS Air Force Systems Command, USAF Andrews AFB Washington, DC 20331		12. REPORT DATE 11 28 Dec 1979	
14. MONITORING AGENCY NAME & ADDRESS (if different from Controlling Office) Electronic Systems Division Hanscom AFB Bedford, MA 01731		13. NUMBER OF PAGES 75	
		15. SECURITY CLASS. (of this report) Unclassified	
		15a. DECLASSIFICATION DOWNGRADING SCHEDULE	
16. DISTRIBUTION STATEMENT (of this Report) Approved for public release; distribution unlimited.			
17. DISTRIBUTION STATEMENT (of the abstract entered in Block 20, if different from Report)			
18. SUPPLEMENTARY NOTES None			
19. KEY WORDS (Continue on reverse side if necessary and identify by block number) PIN diode weight circuits performance design analog feedback processor fabrication adaptive nulling			
20. ABSTRACT (Continue on reverse side if necessary and identify by block number) This report is one of a number of technical notes describing various aspects of the design, fabrication, and performance of a demonstration analog feedback processor. In this report we examine the PIN diode weight circuits which are used in the adaptive processor to control the attenuation and phase of the eight signal channels which make up the processor. The weighting circuits are required to have well-matched transfer functions which track closely from channel to channel so as not to degrade the processor cancellation. To achieve the necessary tracking performance, two different weight circuit designs were investigated. The tracking performance of the first set was found to be limited by the direct feed-through of input signals to the output of the weight circuit as a result of the limited dynamic range of the weight circuit attenuator. To overcome this limitation, a second set of weight circuits having significantly improved tracking characteristics was fabricated using an improved attenuator circuit design. Information relevant to the design, fabrication and testing of each weight circuit is presented along with measured data to demonstrate its performance. Techniques used in characterizing the frequency tracking performance of multiple weight circuits are discussed and measurement data is presented to illustrate the relative tracking performance of the weight circuits.			

DD FORM 1473 EDITION OF 1 NOV 65 IS OBSOLETE
1 JAN 73

UNCLASSIFIED

SECURITY CLASSIFICATION OF THIS PAGE (When Data Entered)

207650